

## Washington University School of Medicine Digital Commons@Becker

---

### Open Access Publications

---

2017

# Viral RNA at two stages of reovirus infection is required for the induction of necroptosis

Angela K. Berger  
*Emory University*

Bradley E. Hiller  
*Washington University School of Medicine*

Deepti Thete  
*Indiana University*

Anthony J. Snyder  
*Indiana University*

Encarnacion Perez Jr  
*University of Texas at Austin*

*See next page for additional authors*

Follow this and additional works at: [https://digitalcommons.wustl.edu/open\\_access\\_pubs](https://digitalcommons.wustl.edu/open_access_pubs)

---

### Recommended Citation

Berger, Angela K.; Hiller, Bradley E.; Thete, Deepti; Snyder, Anthony J.; Perez, Encarnacion Jr; Upton, Jason W.; and Danthi, Pranav, "Viral RNA at two stages of reovirus infection is required for the induction of necroptosis." *The Journal of Virology* 91,6. 1-55. (2017). [https://digitalcommons.wustl.edu/open\\_access\\_pubs/5670](https://digitalcommons.wustl.edu/open_access_pubs/5670)

This Open Access Publication is brought to you for free and open access by Digital Commons@Becker. It has been accepted for inclusion in Open Access Publications by an authorized administrator of Digital Commons@Becker. For more information, please contact [engeszer@wustl.edu](mailto:engeszer@wustl.edu).

---

**Authors**

Angela K. Berger, Bradley E. Hiller, Deepti Thete, Anthony J. Snyder, Encarnacion Perez Jr, Jason W. Upton,  
and Pranav Danthi

1  
2  
3  
4  
5  
6  
7  
8  
9  
10  
11  
12  
13  
14  
15  
16  
17  
18  
19  
20  
21  
22  
23

**Viral RNA at two stages of reovirus infection is required for the  
induction of necroptosis**

Angela K. Berger<sup>1‡</sup>, Bradley E. Hiller<sup>1#</sup>, Deepti Thete<sup>1</sup>, Anthony J. Snyder<sup>1</sup>,  
Encarnacion Perez Jr<sup>2</sup>., Jason W. Upton<sup>2</sup> and Pranav Danthi<sup>1\*</sup>

<sup>1</sup>Department of Biology, Indiana University, Bloomington, Indiana 47405, USA

<sup>2</sup>Department of Molecular Biosciences, LaMontagne Center for Infectious  
Disease, University of Texas, Austin, TX 78712, USA

<sup>\*</sup>, To whom correspondence should be addressed: Department of Biology,  
Indiana University, Bloomington, IN 47405. Tel: 812-856-2449, Fax: 812-856-  
5710, E-mail: [pdanthi@indiana.edu](mailto:pdanthi@indiana.edu)

<sup>‡</sup> Current address: Department of Pediatrics, Emory University School of  
Medicine, Atlanta, GA 30322, USA.

<sup>#</sup> Current address: Washington University in St Louis, 660 South Euclid Ave.  
St. Louis, MO 63110, USA.

24 **ABSTRACT**

25 Necroptosis, a regulated form of necrotic cell death requires the activation of the  
26 RIP3 kinase. Here, we identify that infection of host cells with reovirus can result  
27 in necroptosis. We find that necroptosis requires sensing of the genomic RNA  
28 within incoming virus particles via cytoplasmic RNA sensors to produce type I  
29 IFN. While these events that occur prior to de novo synthesis of viral RNA are  
30 required for induction of necroptosis, they are not sufficient. Induction of  
31 necroptosis also requires late stages of reovirus infection. Specifically, efficient  
32 synthesis of dsRNA within infected cells is required for necroptosis. These data  
33 indicate that viral RNA interfaces with host components at two different stages of  
34 infection to induce necroptosis. This work provides new molecular details about  
35 events in the viral replication cycle that contribute to the induction of necroptosis  
36 following infection with an RNA virus.

37 **IMPORTANCE**

38 An appreciation of how cell death pathways are regulated following viral infection  
39 may reveal strategies to limit tissue destruction and prevent the onset of disease.  
40 Cell death following virus infection can occur by apoptosis or a regulated form of  
41 necrosis, known as necroptosis. Apoptotic cells are typically disposed of without  
42 activating the immune system. In contrast, necroptotic cells alert the immune  
43 system, resulting in inflammation and tissue damage. While apoptosis following  
44 virus infection has been extensively investigated, how necroptosis is unleashed  
45 following virus infection is only understood for a small group of viruses. Here,  
46 using mammalian reovirus, we highlight the molecular mechanism by which  
47 infection with a dsRNA virus results in necroptosis.

48 **INTRODUCTION**

49 Host cell death is a common outcome of virus infection (1). One form of  
50 cell death, necroptosis, has been described following infection with influenza A  
51 virus (IAV), herpes simplex virus 1 and 2 (HSV1 or 2), murine cytomegalovirus  
52 (MCMV), and vaccinia virus (VV). In each of these cases, necroptosis protects  
53 the infected animal (2-7). Examples also exist where increased necroptosis  
54 contributes to tissue injury and exacerbates viral disease (7, 8). The impact of  
55 necroptosis on these viral diseases may be due to premature death of the  
56 infected cell or as a consequence of inflammation induced by leakage of  
57 molecules from necrotic cells (9, 10).

58

59 Necroptosis requires the activation of receptor interacting protein 3 (RIP3)  
60 kinase (6, 11, 12). Once activated, RIP3 kinase signals via the pseudokinase,  
61 mixed lineage kinase-like (MLKL) protein to promote a necrotic form of cell death  
62 that is characterized by loss of membrane integrity and leakage of cellular  
63 contents (13-23). RIP3 contains a receptor-interacting protein homotypic  
64 interacting motif (RHIM) and is activated via interactions with other cellular RHIM-  
65 containing proteins - TRIF (TIR-domain-containing adapter-inducing interferon- $\beta$ ),  
66 RIP1, or DAI (DNA-dependent activator of IFN-regulatory factors) (24). TRIF  
67 activation by Toll-like receptor 3 (TLR3) and TLR4 ligands can evoke necroptosis  
68 but necroptosis by this mechanism has not yet been demonstrated following virus  
69 infection (25, 26). RIP1 activation by tumor necrosis factor  $\alpha$  (TNF $\alpha$ ) induces  
70 RIP3-dependent necroptosis following VV infection (6). The pathogen sensor,

71 DAI is required for necroptosis in cells infected with a MCMV variant (5).  
72 Ribonucleotide reductases, ICP6 and ICP10, respectively encoded by HSV1 and  
73 HSV2 contain a RHIM-like domain. These ribonucleotide reductases interact with  
74 murine RIP1 and RIP3, promote RIP1-RIP3 or RIP3-RIP3 oligomerization, and  
75 induce necroptosis (2, 3).

76

77 In contrast to these studies on DNA viruses, mechanisms by which RNA  
78 viruses induce necroptosis are less understood. IAV induces necroptosis in the  
79 lungs of cIAP2-deficient mice (8). Because uninfected cells also undergo cell  
80 death in this model, it is thought that cell death is a consequence of alteration in  
81 cellular homeostasis rather than induced by viral replication events. In wild-type  
82 cells, IAV activates a RIP3-containing signaling platform that can induce either  
83 apoptosis or necroptosis (7). Recent evidence suggests that DAI, which was  
84 previously thought to be a sensor for cytoplasmic DNA interacts with IAV  
85 components to engage RIP3 and induce necroptosis (27, 28). RNA viruses such  
86 as Coxsackievirus B (CVB), coronavirus, mammalian reovirus (Reovirus),  
87 Theiler's murine encephalomyelitis virus (TMEV), and West Nile virus (WNV)  
88 also have been demonstrated to evoke cell death with morphologic features  
89 resembling necrosis (29-32). However, the events in viral replication that initiate  
90 pronecrotic signaling pathways have not been defined for these RNA viruses.

91

92 In this study, we investigated the mechanism by which reovirus infection  
93 culminates in necroptosis. Our results indicate that IFN $\beta$  produced by detection

94 of genomic RNA of incoming virus particles is required, but not sufficient for  
95 eliciting necroptosis. In addition to IFN $\beta$  expression, de novo synthesis of viral  
96 dsRNA is also required for necroptosis induction. These results suggest that  
97 detection of viral components at two distinct stages is required for the induction  
98 of necroptosis following infection with an RNA virus.



99 **MATERIAL AND METHODS**

100 **Cells and viruses.** Spinner-adapted L929 cells (obtained from Dr. T. Dermody's  
101 laboratory) were maintained in Joklik's MEM (Lonza) supplemented to contain  
102 5% FBS, 2 mM L-glutamine, 100 U/ml of penicillin, 100 µg/mL streptomycin, and  
103 25 ng/mL of amphotericin B. Spinner-adapted L929 cells were used for  
104 cultivating and purifying viruses and for plaque assays. Prototype reovirus strain  
105 T3D was regenerated by plasmid based reverse genetics (33, 34). Viral particles  
106 were purified by Vertrel XF-extraction and CsCl gradient centrifugation (35). Viral  
107 titer was determined by plaque assay using spinner-adapted L929 cells (36). UV-  
108 inactivated virus was generated using a UV cross-linker (CL-1000 UV  
109 Crosslinker; UVP). Virus diluted in PBS was placed in a 60-mm tissue culture  
110 dish and irradiated with short-wave (254-nm) UV on ice at a distance of 10 cm for  
111 1 min at 120,000 µJ/cm<sup>2</sup>. Murine L929 cells (ATCC CCL-1) were maintained in  
112 Eagle's MEM (Lonza) supplemented with 10% fetal bovine serum (FBS), and 2  
113 mM L-glutamine. ATCC L929 cells were used for all experiments to assess cell  
114 death, viral RNA and protein synthesis, and cell signaling. Distinct from some  
115 L929 cell lines, the ATCC L929 cells used for this study do not undergo TNF $\alpha$  or  
116 zVAD-mediated cell death (37, 38). Wild-type and mutant bone marrow derived  
117 macrophages were obtained from Drs. Edward Mocarski and Mehul Suthar  
118 (Emory University) and were maintained in DMEM with 20% FBS, 10% filtered  
119 conditioned medium from L929 cells, 2 mM L-glutamine, 100 U/ml of penicillin,  
120 and 100 µg/mL streptomycin.  
121

122 **Reagents.** Z-VAD-FMK and Q-VD-OPh were purchased from Enzo Life  
123 Sciences or R & D Systems, Necrostatin-1 was purchased from Calbiochem.  
124 Ammonium chloride (AC), GuHCl, poly I:C, and human TNF $\alpha$  were purchased  
125 from Sigma-Aldrich. siRNAs were purchased from Dharmacon as SMARTpools  
126 of ON-TARGET plus siRNA. Non-targeting siRNA control pool or siRNA targeting  
127  $\beta$ -galactosidase were used as controls. Antisera raised against reovirus were  
128 obtained from T. Dermody. Monoclonal antibody against IFNAR and rabbit  
129 antisera against RIP3 were purchased from Santa Cruz Biotechnology, those  
130 against TRIF, phospho-MLKL and total MLKL were purchased from Abcam, and  
131 those against RIG-I and MDA5 were purchased from Cell Signaling. Mouse  
132 antiserum specific for PSTAIR was purchased from Sigma, specific for KDEL  
133 was purchased from Enzo Life Sciences. Alexa Fluor-conjugated anti-mouse  
134 IgG, anti-rabbit IgG, and anti-goat IgG secondary antibodies were purchased  
135 from Invitrogen. IRDye-conjugated anti-guinea pig IgG was purchased from LI-  
136 COR.

137

138 **Fixing, embedding, and sectioning of infected cells.** L929 cells grown on 100  
139 mm dishes were either mock infected or infected with 10 PFU/cell of T3D for 1 h  
140 at room temperature. Following the viral attachment incubation, the cells were  
141 washed twice with PBS and then overlaid with fresh medium. At 34 h post  
142 infection, uninfected and infected cells were washed with PBS, trypsinized,  
143 pelleted for 5 min at 800  $\times$  g, and washed again with PBS. The pelleted cells  
144 were then fixed with 2.5% glutaraldehyde diluted in sodium cacodylate buffer

145 (100 mM sodium cacodylate [pH 7.5], 2 mM MgCl<sub>2</sub>, 2 mM CaCl<sub>2</sub>, 0.5% NaCl) for  
146 60 min at room temperature. Following fixation, the cells were washed twice with  
147 sodium cacodylate buffer. The washed cells were post fixed with 1% osmium  
148 tetroxide diluted in sodium cacodylate buffer for 60 min at room temperature.  
149 The fixed cells were washed twice with sodium cacodylate buffer followed by one  
150 wash with 100 mM sodium acetate [pH 4.2]. The cells were then stained with  
151 0.5% uranyl acetate diluted in 100 mM sodium acetate [pH 4.2] for 60 min at  
152 room temperature. After staining, the cells were washed twice with 100 mM  
153 sodium acetate [pH 4.2]. Prior to embedding, the fixed and stained cells were  
154 dehydrated with sequential concentrations of ethanol (EtOH): 35% EtOH once  
155 for 5 min, 50% EtOH once for 5 min, 70% EtOH once for 5 min, 90% EtOH once  
156 for 5 min, 95% EtOH once for 5 min, and 100% EtOH four times for 5 min each.  
157 The dehydrated cells were incubated in a solution composed of 50% EMbed 812  
158 resin and 50% EtOH for 2 h at room temperature. The cells were then incubated  
159 in 100% EMbed 812 resin overnight at room temperature. The next day, the  
160 resin was replaced with fresh EMbed 812 resin, which was allowed to harden for  
161 18 h at 65°C. Thin-sections (85 nm thick) were collected using a diamond knife  
162 on a Leica Biosystems microtome.

163

164 **Transmission electron microscopy (TEM).** Thin-sections of uninfected and  
165 infected cells were applied to 300-mesh copper grids and stained with Reynold's  
166 lead citrate and 2% uranyl acetate (40). The stained grids were analyzed using a  
167 JEOL 1010 transmission electron microscope operating at 80 kV. Images were

168 recorded using a Gatan MegaScan 794 charge-coupled-device camera.

169 Micrographs were processed and analyzed using ImageJ software.

170

171 **Infections and preparation of extracts.** Cells were either adsorbed with PBS or

172 T3D at room temperature for 1 h, followed by incubation with media at 37°C for

173 the indicated time interval. Ribavirin, GuHCl, Z-VAD-FMK, Q-VD-OPh,

174 Necrostatin-1, or anti-IFNAR Ab was added to the media immediately after the 1

175 h adsorption period. For preparation of whole cell lysates, cells were washed in

176 phosphate-buffered saline (PBS) and lysed with 1X RIPA (50 mM Tris [pH 7.5],

177 50 mM NaCl, 1% TX-100, 1% DOC, 0.1% SDS, and 1 mM EDTA) containing a

178 protease inhibitor cocktail (Roche), 500  $\mu$ M DTT, and 500  $\mu$ M PMSF, followed by

179 centrifugation at 15000  $\times$  g for 10 min to remove debris. For detection of

180 phosphorylated MLKL, cells were lysed in 1X RIPA supplemented with 10 mM

181 NaF.

182

183 **RNA transfection and cell death.** L929 cells were mock infected or infected

184 with 10 PFU/cell of T3D for 24 h. Total RNA was extracted using Tri-reagent

185 (Molecular Research Center). When needed, the RNA was mock treated or CIP

186 treated for 1 h at 37°C and repurified using Tri-reagent. 100 ng of RNA was

187 introduced into the cells by Lipofectamine 2000 transfection. Cell death was

188 measured 21-24 h following transfection.

189

190 **Immunoblot assay.** Cell lysates were resolved by electrophoresis in  
191 polyacrylamide gels and transferred to nitrocellulose membranes. Membranes  
192 were blocked for at least 1 h in blocking buffer (PBS containing 5% milk or 2.5%  
193 BSA) and incubated with antisera against MLKL (1:2000), phospho-MLKL (1:750),  
194 RIP3 (1:1000), MAVS (1:1000), RIG-I (1:1000), MDA5 (1:1000), TRIF (1:1000),  
195 or PSTAIR (1:10000) at 4°C overnight. Membranes were washed three times for  
196 5 min each with washing buffer (TBS containing 0.1% Tween-20) and incubated  
197 with 1:20000 dilution of Alexa Fluor conjugated goat anti-rabbit IgG (for RIP3,  
198 RIG-I, and MDA5), donkey anti-goat IgG (for RIP3), goat anti-mouse IgG (for  
199 KDEL and PSTAIR), or IRDye-conjugated anti-guinea pig IgG (for  $\sigma$ NS) in  
200 blocking buffer. Following three washes, membranes were scanned using an  
201 Odyssey Infrared Imager (LI-COR).

202  
203 **Knockdown of host proteins by siRNA.** In 96-well plates, 0.25  $\mu$ l  
204 Lipofectamine 2000 was used to transfect 15 pmoles of siRNA. Cells ( $1 \times 10^4$ )  
205 were seeded on top of the siRNA-lipofectamine mixture. In 24-well plates, 0.75  $\mu$ l  
206 Lipofectamine 2000 was used to transfect 45 pmoles of siRNA. Cells ( $5 \times 10^4$ )  
207 were seeded on top of the siRNA-lipofectamine mixture. Virus infection was  
208 performed 48 h following siRNA transfection.

209  
210 **Assessment of cell death by measuring cellular ATP levels.** Cells ( $1 \times 10^4$ )  
211 grown in black, clear-bottom 96-well plates were mock infected with PBS or  
212 adsorbed with 10 PFU/cell of T3D at room temperature for 1 h. Following

213 incubation of cells at 37°C for 42 h, ATP levels were assessed using the Cell  
214 titer-Glo assay system (Promega).

215

216 **Assessment of cell death by acridine orange ethidium bromide staining.**

217 Cells grown in 24-well plates or 96-well plates were adsorbed with the indicated  
218 amount of virus. Inhibitors were added immediately following adsorption. The  
219 percentage of dead cells after 48 h incubation was determined using AOEB  
220 staining as described (41). For identifying host regulators of cell death, cells were  
221 transfected with siRNA as described above and incubated for 48 h prior to  
222 infection with T3D. For each experiment, >250 cells were counted by a blinded  
223 researchers, and the percentage of isolated cells exhibiting orange staining (EB  
224 positivity) was determined by epi-illumination fluorescence microscopy using a  
225 fluorescein filter set on an Olympus IX71 microscope. < 5% of uninfected cells  
226 were EB positive following treatment with each inhibitor or siRNA.

227

228 **Assessment of cell death by IncuCyte automated cell imaging.** Cells grown

229 in 48-well plates were mock infected with PBS or adsorbed with the indicated  
230 amount of virus. Inhibitors were added immediately following adsorption in  
231 addition to 500 nM Sytox green. The cells were imaged over a time course of 48  
232 h. Values of Sytox positive cells per mm<sup>2</sup> 48 h following infection are shown.

233

234 **Assessment of caspase-3/7 activity.** ATCC L929 cells ( $1 \times 10^4$ ) were seeded

235 into black clear-bottom 96-well plates, adsorbed with 10 PFU/cell of reovirus in

236 serum-free medium at room temperature for 1 h. Following incubation of cells at  
237 37°C for 48 h, caspase-3/7 activity was quantified using the Caspase-Glo-3/7  
238 assay system (Promega).

239

240 **Assessment of viral yield.** BMDMs in 24-well plates were adsorbed in triplicate  
241 with 50 PFU/cell of T3D for 1 h. Cells were washed once with PBS, and  
242 incubated for 0 h or 24 h. Cells were frozen and thawed twice prior to  
243 determination of viral titer by plaque assay. Viral yields were calculated according  
244 to the following formula:  $\log_{10}\text{yield}_{24\text{h}} = \log_{10}(\text{PFU/ml})_{24\text{h}} - \log_{10}(\text{PFU/ml})_{0\text{h}}$ .

245

246 **RT-qPCR.** RNA was extracted from infected cells at various time intervals after  
247 infection using Tri-reagent or an RNAeasy kit (Qiagen). For RT-qPCR, 0.5 to 2  
248  $\mu\text{g}$  of RNA was reverse transcribed using random hexamers or gene specific  
249 primers using High Capacity cDNA Reverse Transcription Kit (Applied  
250 Biosystems). A 1:10 dilution of the cDNA was subjected to PCR using SYBR  
251 Select Master Mix (Applied Biosystems).  $\Delta\text{Ct}$  values for each cDNA sample were  
252 calculated by subtracting Ct values of T3DS1, ZBP1, or IFN $\beta$  and Ct values for  
253 GAPDH. Fold increase in gene expression with respect to control sample  
254 (indicated in each figure legend) was measured using the  $\Delta\Delta\text{Ct}$  method (42).

255

256 **Statistical analysis.** Statistical significance between experimental groups was  
257 determined using the unpaired *t*-test function of the Graphpad Prism software.

258 Statistical analyses for differences in gene expression by RT-qPCR were done  
259 on the  $\Delta C_t$  values.  
260



261 **RESULTS**

262 **Reovirus-induces necroptosis.** Upon ultrastructural evaluation of L929 cells  
263 infected with prototype reovirus strain Type 3 Dearing (T3D) 34 h following  
264 infection (a time point conducive for recovery and processing of dying cells for  
265 microscopy), we observed cells with normal nuclear morphology, the absence of  
266 apoptotic blebs, swelling of the cellular cytoplasm and early stages of disruption  
267 of the plasma membrane (Figure 1A). These features are not characteristic of  
268 apoptosis and suggested that reovirus may elicit an alternate form of cell death,  
269 such as necrosis. Cell death can be assessed by measurement of cellular ATP  
270 levels or by evaluating the permeability of cellular nuclei to DNA-staining vital  
271 dyes. These treatments do not distinguish between cell death by apoptosis or  
272 necrosis and therefore need to be coupled with pharmacologic blockade of  
273 molecules specifically involved in cell death pathways leading to apoptosis or  
274 necrosis (43). Consistent with the absence of apoptotic features, although  
275 pancaspase inhibitors Z-VAD-FMK or Q-VD-OPh abolish effector caspase  
276 activation in L929 cells infected with reovirus, they fail to block cell death (Figure  
277 1B and 1C) (30). Instead, cell death following reovirus infection of L929 cells  
278 exhibits features of necrosis and is diminished by Nec1, a RIP1 kinase inhibitor  
279 (30). The kinase activity of RIP1 can potentiate the activation of RIP3 to promote  
280 necroptosis (6). To determine if reovirus-induced cell death occurs via this  
281 mechanism, we assessed the capacity of reovirus to elicit necrosis in cells  
282 expressing reduced levels of RIP3 (Figure 1D). We found that in comparison to  
283 cells treated with control siRNA, treatment of cells with siRNAs against RIP3

284 significantly decreased cell death (Figure 1E, 1F). The effect of RIP3 siRNA  
285 against reovirus-induced cell death matched the effect of RIP3 siRNA on  
286 necroptosis-inducing treatment of TNF $\alpha$  and Z-VAD-FMK (Figure 1G). These  
287 data indicate a role for RIP3 in the induction of cell death following reovirus  
288 infection. RIP3 can participate in the induction of both apoptosis and necroptosis  
289 (7, 44, 45). Because cell death following reovirus infection is unaffected by  
290 diminishment of caspase activity (Figure 1B, 1C), these data suggest that reovirus  
291 induces RIP3-dependent necroptosis in L929 cells.

292           RIP3-dependent necroptosis requires the activation of the effector protein  
293 MLKL (13-23). MLKL is directly phosphorylated by RIP3 and MLKL  
294 phosphorylation is considered to be a hallmark of the activation of necroptosis  
295 signaling cascade (13, 46). To determine if reovirus infection leads to the  
296 activation of MLKL, we immunoblotted extracts from reovirus-infected cells using  
297 a phospho-MLKL antibody (Figure 1H). Our results indicate that MLKL is  
298 activated within 24 h following reovirus infection and remains activated until 48 h  
299 post infection, when a significant proportion of cells are undergoing cell death.  
300 The detection of this biochemical marker along with the genetic and  
301 pharmacologic experiments described above indicating that cell death is blocked  
302 by loss of RIP3 function but not of caspase function, meet the criteria to  
303 demonstrate that reovirus infection of L929 cells results in necroptosis (15).

304

305           Reovirus infects cells in a variety of tissues in newborn mice. Previous  
306 work on reovirus-induced apoptosis has utilized primary neurons or mouse

307 embryo fibroblasts (MEFs) to evaluate cell death pathways in primary cells. Since  
308 both neurons and MEFs succumb to reovirus via apoptosis (47-54), we used  
309 bone marrow-derived macrophages (BMDMs) to determine whether reovirus can  
310 induce necroptosis in primary cells. While it is not known if cells within the bone  
311 marrow are infected in reovirus-infected animals, identification of primary cells  
312 that undergo necroptosis following reovirus infection would allow us to  
313 complement our siRNA studies with work in cells from mice genetically deficient  
314 in important regulators of necroptosis. We found that cell death following reovirus  
315 infection of BMDMs occurred in the absence of caspase activity (Z-VAD-FMK-  
316 treated cells) or RIP1 kinase activity (Nec1-treated cells) but was diminished  
317 when the activity of caspases and RIP1 kinase were simultaneously blocked  
318 (Figure 2A). Consistent with this, cell death was not blocked by the genetic  
319 absence of RIP3 but was reduced by blockade of caspases in the absence of  
320 RIP3 (Figure 2B, 2C). Cells lacking both caspase-8 and RIP3 were also resistant  
321 to death following reovirus infection (Figure 2D). These data indicate that  
322 reovirus can induce necroptosis in BMDMs when apoptosis is blocked. These  
323 findings match previous work in other systems where necroptosis is evident  
324 when caspases have been rendered non-functional (55-57).

325         In the context of infection by other viruses, necroptosis is antiviral (2, 4-7).  
326 To determine if necroptosis affects replication of reovirus, we measured viral  
327 yield over 24 h of infection in wild-type and RIP3-deficient BMDMs in the  
328 presence and absence of Z-VAD-FMK. Viral yields in wild-type cells treated with  
329 DMSO or Z-VAD-FMK were  $\sim 1 \log_{10}$  (Figure 2E). The genetic absence of RIP3

330 enhanced viral yield to  $\sim 1.7 \log_{10}$ . Importantly, viral yield did not change in RIP3-  
331 deficient BMDMs in conditions where apoptosis was blocked using Z-VAD-FMK.  
332 While the basis for the slight increase in viral yield in absence of RIP3 is unclear  
333 and was not further investigated, our data suggest that the capacity of cells to  
334 undergo necroptosis does not influence viral yield in cell culture. These data are  
335 reminiscent of previous evidence indicating that blockade of apoptosis does not  
336 influence reovirus replication in cell culture (47, 48). The absence of effect of cell  
337 death on reovirus replication in cell culture may be due to the differences in  
338 timing of the reovirus replication cycle and the induction of cell death. Whereas  
339 reovirus completes its replication cycle in 18 h, cell death following infection is  
340 not detected until 36-48 h following infection.

341

342 **Transfection of reovirus RNA can elicit necroptosis.** Reovirus strains that  
343 exhibit a greater level of gene expression are more potent inducers of necrosis  
344 (58). Blockade of reovirus + strand RNA synthesis using ribavirin blocks necrosis,  
345 suggesting a possible role for viral RNA in the induction of necrosis (58).  
346 Transfection of dsRNA mimic poly I:C in L929 cells treated with either type I or  
347 type II IFNs results in cell death by necrosis (25, 26, 59). Because our data  
348 suggested a role for reovirus RNA in the induction of necroptosis in infected cells,  
349 we sought to determine if viral RNA was sufficient for the induction of  
350 necroptosis. For these experiments, we purified total RNA from mock- or  
351 reovirus-infected cells 24 h following infection. We found that in comparison to  
352 RNA from mock-infected cells, RNA extracted from T3D-infected cells induced a

353 significantly greater amount of cell death following transfection into cells (Figure  
354 3A, 3B). Cell death by transfected RNA was diminished by treatment with Nec1  
355 but not Q-VD-OPh (Figure 3C), analogous to what we have reported in L929  
356 cells infected with reovirus (30). These data are also consistent with previous  
357 work indicating that poly I:C-induced cell death is blocked by Nec1 (26). Our  
358 results presented above suggest that RNA isolated from reovirus-infected cells  
359 elicits necroptosis following introduction into L929 cells. Interestingly, unlike  
360 previous work with transfection of dsRNA into cells (25, 59), cell death following  
361 transfection of RNA extracted from reovirus-infected cells did not require priming  
362 of the cells with exogenous IFN.

363 We reasoned that necroptosis was induced without addition of exogenous  
364 IFN because transfection of reovirus RNA obtained from infected cells can  
365 induce the expression of IFN $\beta$  (60-62)(Figure 3D). Indeed, treatment with an  
366 IFNAR-blocking antibody MAR1-5A3 (63), resulted in a reduction in cell death  
367 (Figure 3D). IFN $\beta$  production following transfection of reovirus RNA occurs via  
368 RIG-I-mediated detection of the RNA (60). Consistent with this, removal of the 5'  
369 phosphates using CIP resulted in a reduction in the expression of IFN $\beta$  (Figure  
370 3E) and the induction of cell death (Figure 3F, 3G). Interestingly, if cells were  
371 primed with exogenous IFN $\beta$  before transfection, the capacity of CIP-treated  
372 RNA to elicit necroptosis was restored (Figure 3F, 3G). These data suggest that  
373 though RIG-I mediated detection of viral RNA is required for IFN $\beta$  production, it is  
374 not sufficient for the induction of cell death. Thus, cell death induction occurs by  
375 sensing of viral RNA via an alternate pathway.

376           Based on the evidence that poly I:C elicits necroptosis by TLR3 detection  
377 and signaling to RIP3 via TRIF (25, 26), we examined whether reovirus RNA-  
378 induced necroptosis could be blocked by treatment of cells with ammonium  
379 chloride (AC), an agent that blocks TLR3-mediated detection of dsRNA (64). We  
380 found that though AC did not negatively impact IFN $\beta$  expression following RNA  
381 transfection (Figure 3H), it blocked cell death induction by transfected RNA  
382 (Figure 3I). Consistent with previous work, these data indicate that detection of  
383 reovirus RNA via RIG-I produces IFN $\beta$ . In addition, these data suggest that IFN $\beta$   
384 primes reovirus RNA transfected cell to undergo TLR3-dependent necroptosis.  
385 Thus, the IFN- and TLR3-dependent pathway for induction of necroptosis  
386 following transfection of reovirus RNA into L929 cells is similar to that previously  
387 described for transfection of synthetic dsRNA (25, 59).

388

389 **Sensing of reovirus RNA during infection is required for necroptosis.** We  
390 next sought to determine if detection of viral RNA in infected cells contributes to  
391 cell death induction in reovirus-infected cells. During infection, reovirus RNA can  
392 be detected by both RIG-I-like receptors (RLRs), RIG-I and MDA5 (65).  
393 Simultaneous reduction of both RLRs, or their common downstream signaling  
394 adaptor, MAVS, led to a significant reduction in cell death following reovirus  
395 infection (Figure 4A, 4B, 4C). The susceptibility of cells to TNF $\alpha$  and Z-VAD-FMK  
396 induced necroptosis was not changed following MAVS knockdown indicating that  
397 MAVS is not required for the function of the core necroptosis machinery (Figure  
398 4D). BMDMs deficient in either both RLRs or MAVS were also protected from

399 reovirus-induced necroptosis (Figure 4E, 4F). These data suggest that  
400 necroptosis following reovirus infection requires detection and signaling by RLRs.

401

402 **IFN signaling is required for necroptosis.** To determine whether type I IFNs  
403 produced by RLR-MAVS signaling are required for reovirus-induced necroptosis,  
404 we quantified the capacity of reovirus to induce necroptosis in the presence of an  
405 IFNAR-blocking antibody (63). We found that this antibody diminished the  
406 expression of a representative interferon-stimulated gene (ISG), ZBP1, which is  
407 potently induced following reovirus infection (66), and diminished the capacity of  
408 reovirus to induce necroptosis (Figure 5A, 5B, 5C). This reduction in necroptosis  
409 was not due to a deleterious effect of the antibody on the capacity of reovirus to  
410 establish infection (Figure 5D). Blocking IFNAR signaling did not alter the  
411 capacity of TNF $\alpha$  and Z-VAD-FMK cotreatment to induce necroptosis, suggesting  
412 that this treatment did not affect the function of the core necroptosis machinery  
413 (Figure 5E). IFNAR-deficient BMDMs treated with Z-VAD-FMK also were  
414 resistant to reovirus-induced necroptosis (Figure 5E, 5F), indicating a role for IFN  
415 signaling in the induction of necroptosis following reovirus infection.

416       Based on the role for TLR3 in necroptosis following transfection of RNA  
417 obtained from reovirus-infected cells (Figure 3), we next sought to evaluate  
418 whether TLR3 is also required for cell death in reovirus-infected cells. Toward  
419 this goal, we tested the effect of AC on cell death induction in reovirus-infected  
420 cells. Because treatment of cells with AC prevents reovirus infection by blocking  
421 capsid disassembly, we initiated infection of AC-treated cells with infectious

422 subviral particles (ISVPs), a viral entry intermediate that bypasses the inhibitory  
423 effect of AC (67). We found that necroptosis following infection by ISVPs was  
424 unaffected by treatment with AC (Figure 5G). Parallel transfection of cells with  
425 reovirus RNA in control and AC treated cells yielded results that matched those  
426 described in Figure 3H (data not shown), indicating that AC treatment was  
427 effective. siRNA-mediated reduction in the expression of TRIF, the TLR3 adaptor  
428 also did not block cell death following reovirus infection (Figure 5H, 5I). These  
429 data indicate that although RLR-mediated IFN $\beta$  expression and signaling is  
430 required for necroptosis following both, RNA transfection and viral infection,  
431 TLR3-mediated signaling is only required for cell death after viral RNA  
432 transfection.

433

434 **Two-stage detection of reovirus infection is required for necroptosis.**

435 We next sought to determine the stage of infection required for the induction of  
436 necroptosis. Blockade of viral + strand RNA synthesis using ribavirin diminishes  
437 reovirus-induced necrosis (58). The reovirus + sense RNA can direct protein  
438 synthesis or can be packaged into progeny core particles and serve as the  
439 template for minus strand RNA synthesis to generate viral genomic dsRNA (68).  
440 Progeny cores containing genomic dsRNA undergo secondary transcription to  
441 produce additional viral mRNAs. Thus, the diminishment of necroptosis by  
442 ribavirin treatment may be due to blockade of any of these steps in reovirus  
443 replication. To define the stage of infection required for necroptosis further, we  
444 used Guanidine hydrochloride (GuHCl). GuHCl does not affect reovirus + strand



445 RNA synthesis but prevents the generation of genomic dsRNA within infected  
446 cells (Figure 6A, 6C)(69). Under the conditions used, perhaps because sufficient  
447 translation occurs from primary transcripts, we did not observe a diminishment in  
448 viral protein synthesis in the presence of GuHCl (Figure 6B). Treatment of  
449 reovirus-infected cells with GuHCl led to diminishment in necroptosis (Figure 6D,  
450 6E). Because GuHCl does not affect necroptosis induced by TNF $\alpha$  and Z-VAD-  
451 FMK treatment (Figure 6F), our results point to the importance of the synthesis of  
452 viral genomic dsRNA for the induction of necroptosis following reovirus infection.

453         It is not known when during infection reovirus RNA is detected to produce  
454 IFN $\beta$ . The type of reovirus RNA that activates the expression of IFN $\beta$  in the  
455 context of infection also remains undefined. Ribavirin and GuHCl may thus  
456 indirectly prevent cell death because they affect the synthesis of RNA required  
457 for IFN $\beta$  synthesis. To better understand the effect of ribavirin and GuHCl on  
458 reovirus-induced cell death, we measured the expression of the IFN $\beta$  mRNA at  
459 different times following infection of L929 cells with reovirus. We observed a ~ 10  
460 fold increase in IFN $\beta$  mRNA levels 12 h following infection (Figure 7A). No further  
461 increase in IFN $\beta$  mRNA was observed at 18 or 24 h following infection. We found  
462 that though IFN $\beta$  mRNA expression was diminished by blockade of virus  
463 disassembly using AC, it was not decreased by either ribavirin or GuHCl  
464 treatment (Figure 7B). Although UV-inactivated virus failed to produce detectable  
465 levels of reovirus S1 + strand RNA (> 3 log<sub>10</sub>-fold reduction), it remained capable  
466 of eliciting the same level of IFN $\beta$  mRNA expression as control, infectious virus  
467 (Figure 7C, 7D). These data suggest that genomic RNA present within incoming

468 viral particles is sufficient for the induction of IFN $\beta$  expression. These results are  
469 consistent with data describing IFN induction by a UV inactivated reovirus  
470 mutant, IRF3 activation following reovirus infection in absence of RNA synthesis  
471 and recent studies on IFN expression following avian reovirus infection (49, 70,  
472 71). We observed that an infection-induced increase in IFN $\beta$  expression was  
473 diminished in cells transfected with MAVS siRNA (Figure 7E). Importantly, MAVS  
474 was also required for efficient induction of IFN $\beta$  expression in reovirus-infected  
475 cells when viral + strand RNA synthesis was blocked using ribavirin (Figure 7E).  
476 These data suggest that genomic RNA within incoming virus particles is detected  
477 by cytoplasmically localized RLRs and signals via MAVS to produce IFN $\beta$ .  
478 Because necroptosis is blocked by GuHCl under conditions where IFN $\beta$  is  
479 produced but viral dsRNA synthesis is diminished (Figure 6, 7), these studies  
480 indicate that IFN $\beta$  signaling is required but not sufficient for the induction of cell  
481 death. Together, our data indicate a role for reovirus RNA at two different stages  
482 of infection to induce necroptosis. First, viral genomic dsRNA is detected during  
483 entry to activate type I IFN signaling. Second, generation of newly synthesized  
484 viral dsRNA is required for the induction of necroptosis.

485 **DISCUSSION**

486 In this manuscript, we demonstrate that reovirus infection of both cultured cells  
487 and primary murine macrophages evokes necroptosis. Our results point to a role  
488 for viral components at two stages of infection to evoke necroptosis (Figure 8).  
489 First, detection of the incoming viral genomic RNA by host cell cytoplasmic  
490 sensors to produce IFN $\beta$  is required for necroptosis (Figure 4). In addition,  
491 synthesis of new viral genomic dsRNA also is required for the induction of  
492 necroptosis (Figure 6). This work indicates that the type I IFN signaling pathway  
493 functions in the induction of necroptosis following infection by an RNA virus.  
494 These data provide evidence for a previously unknown signaling cascade by  
495 which infection with an RNA virus culminates in necroptosis.

496 IFN signaling has been previously implicated in the induction of  
497 necroptosis. In *Salmonella typhimurium* infected mice, murine macrophages  
498 undergo necroptosis (72). In this context, the IFNAR is internalized and  
499 complexes with RIP1 and RIP3 to elicit necroptosis (72). ISGF3, a protein  
500 complex that drives the expression of ISGs following IFN signaling is required for  
501 sustained activation of RIP3 following ligation of TNFR or TLRs (73). However,  
502 whether a particular ISG modulates the basal activity of RIP3 has not been  
503 defined. Multiple ISGs are implicated in the induction of necroptosis. These  
504 include ZBP1/DAI, which may sense either viral DNA, viral RNA, or viral proteins,  
505 and those that recognize viral dsRNA (TLR3 and PKR)(5, 25, 27, 28, 74). Based  
506 on the role of DAI in the induction of necroptosis following IAV infection (27, 28),  
507 we tested the contribution of DAI to reovirus induced cell death. We found that

508 reovirus remained capable of inducing cell death in ZBP1-deficient BMDMs (data  
509 not shown). Our results suggest that TLR3 does not participate in necroptosis  
510 induction following reovirus infection (Figure 5). PKR can promote necroptosis in  
511 cells lacking functional FADD (74). Reovirus induces necroptosis in wild-type  
512 cells expressing FADD (Figure 1, 2). Moreover, because reovirus encodes a  
513 well-described PKR inhibitor, we think it unlikely that PKR is involved in this  
514 process (75). Thus, the identity of the ISGs that control necroptosis following  
515 reovirus infection remains to be determined. Because IAV induced necroptosis is  
516 unaffected by the genetic absence of MAVS or IFNAR (7) and requires ZBP1  
517 (27, 28), whereas reovirus-induced necroptosis requires MAVS and IFNAR  
518 (Figure 4, 5) but is not affected by the absence of ZBP1, the mechanism  
519 underlying necroptosis following reovirus infection appears distinct from that  
520 reported for IAV.

521           Investigations into reovirus-induced cell death indicate that reovirus  
522 infection can initiate cell death signaling from distinct stages of replication and  
523 elicit cell death via a variety of pathways. The precise pathway that executes cell  
524 death likely varies with cell type. One model suggests that events initiated during  
525 cell entry that occur after virus disassembly but prior to de novo synthesis of viral  
526 RNA and proteins can elicit cell death by apoptosis (76). Apoptosis by this  
527 mechanism is thought to occur independently of the presence of viral genomic  
528 RNA but relies on the function of the  $\mu$ 1 capsid protein and the host transcription  
529 factor NF $\kappa$ B (47, 77). Another set of studies implicates a role for viral genomic  
530 RNA, viral RNA sensors, and IRF3 in the induction of apoptosis. However, cell

531 death by this pathway does not appear to require viral replication or type I IFN  
532 signaling (49, 78). Two BH3-only members of the Bcl-2 family, Bid and Noxa  
533 appear to be involved in the induction of apoptosis and their function is  
534 downstream of transcription factors NF $\kappa$ B and IRF3 (48, 78). Our studies  
535 presented highlight an additional way in which reovirus infection leads to cell  
536 death. First, distinct from previous work on reovirus-induced apoptosis, we show  
537 that IFN signaling is required for necroptosis. Though we have not directly tested  
538 its requirement, IRF3, which is required for IFN $\beta$  expression (79), likely also plays  
539 a role in necroptosis. Thus the requirement for IRF3 in reovirus induced  
540 apoptosis and necroptosis is likely shared. Unlike for apoptosis, we demonstrate  
541 that the generation of viral genomic dsRNA late in infection is required for  
542 necroptosis (Figure 5). The requirement for genomic dsRNA synthesis may be  
543 direct, similar to the detection of viral RNA during transfection (Figure 2).  
544 Alternatively, synthesis of genomic dsRNA may be required to produce  
545 secondary transcripts, which in turn are detected by the host cell to induce  
546 necroptosis. Secondary transcripts generated following reovirus infection are  
547 qualitatively different than primary transcripts, and therefore, it is possible that  
548 secondary transcripts are detected in a manner distinct from primary transcripts  
549 (80). Though our studies indicate that protein synthesis in absence of ongoing  
550 dsRNA synthesis is not sufficient for necroptosis induction (Figure 6), it remains  
551 possible that viral proteins modulate necroptosis following reovirus infection.

552 Studies thus far have indicated a pathogenic role for apoptosis in reovirus-  
553 induced encephalitis and myocarditis (81). Cell death pathways in reovirus-

554 infected animals are thought to be tissue specific but precisely how these cell  
555 death pathways differ in a tissue-specific manner has not been defined (82, 83).  
556 It is possible that in some cases, cell death via IFN-dependent pathways we have  
557 described in this study contribute to tissue injury. Due to its natural preference for  
558 infecting and killing transformed cells and its innocuousness to human adults,  
559 reovirus is currently in phase III clinical trials as a cancer therapeutic (84). The  
560 capacity of reovirus to elicit cell death via multiple mechanisms may therefore  
561 underlie its efficacy as an effective therapeutic.

562 **ACKNOWLEDGMENTS**

563 We are grateful to Bernardo Mainou, Indiana University Virology colleagues, and  
564 members of our laboratory for helpful discussions and review of the manuscript.

565 Transmission electron microscopy was performed in the Indiana University

566 Bloomington Electron Microscopy Center with assistance of Dr. Barry Stein.

567 **FIGURE LEGENDS**

568 **Figure 1. Reovirus-induces necroptosis in L929 cells.** (A) L929 cells infected  
569 with 10 PFU/cell of T3D for 34 h were fixed, stained, and imaged using  
570 transmission electron microscopy. (B) Cell death in L929 cells 48 h following  
571 mock infection or infection with 10 PFU/cell of T3D and treatment with DMSO or  
572 Q-VD-OPh (20  $\mu$ M) was assessed by Cell Titer Glo. Luminescence measurement  
573 in similarly treated, uninfected cells was considered to represent 100% viability.  
574 (C) Caspase-3/7 activity 48 h following infection of L929 cells with 10 PFU/cell of  
575 T3D and treatment with DMSO or Q-VD-OPh was assessed by a  
576 chemiluminescent enzymatic assay. Caspase activity in mock-infected cells was  
577 set to 1. Data are represented as relative caspase-3/7 activity in comparison to  
578 similarly treated, uninfected cells. \*,  $P < 0.05$  compared to cells treated with  
579 DMSO. (D, E, F, G) L929 cells were transfected with non-targeting siRNAs or  
580 siRNAs specific for RIP3 (D) Efficiency of knockdown was assessed by  
581 immunoblotting for RIP3 and PSTAIR loading control. (E) Cell death 48 h  
582 following mock infection or infection with 10 PFU/cell of T3D was assessed by  
583 Cell Titer Glo. Luminescence measurement in similarly treated, uninfected cells  
584 was considered to represent 100% viability. \*,  $P < 0.05$  compared to cells  
585 transfected with non-targeting siRNAs. (F) Cell death 48 h following infection with  
586 10 PFU/cell of T3D was assessed by AOEB staining. \*,  $P < 0.05$  compared to  
587 cells transfected with non-targeting siRNAs. (G) Cell death 3 h following  
588 treatment with  $TNF\alpha$  and Z-VAD-FMK treatment was assessed by Cell Titer Glo.  
589 Luminescence measurement in similarly siRNA treated, DMSO treated cells was



590 considered to represent 100% viability. (H) Whole cell extracts from L929 cells  
591 infected with 10 PFU/cell of T3D at the indicated time points were immunoblotted  
592 for phosphorylated MLKL, total MLKL, and PSTAIR loading control.

593

594 **Figure 2. Reovirus can induce necroptosis in primary BMDMs.** (A) BMDMs  
595 from wild-type mice were mock infected or infected with 50 PFU/cell of T3D in the  
596 presence of DMSO, Z-VAD-FMK (25  $\mu$ M) or Nec1 (50  $\mu$ M) or both inhibitors. Cell  
597 death 48 h following infection was assessed by Cell Titer Glo. Luminescence  
598 measurement in similarly treated, uninfected cells was considered to represent  
599 100% viability. \*,  $P < 0.05$  compared to DMSO treated cells. (B) BMDMs from  
600 wild-type (left panel) or RIP3  $-/-$  (right panel) mice were mock infected or infected  
601 with 50 PFU/cell of T3D in the presence DMSO or Z-VAD-FMK (25  $\mu$ M). Cell  
602 death 48 h following infection was assessed by Cell Titer Glo. Luminescence  
603 measurement in uninfected cells of the same genotype that were similarly treated  
604 was considered to represent 100% viability. \*,  $P < 0.05$  compared to DMSO  
605 treated cells of the same genotype. (C) BMDMs were infected with 50 PFU/cell of  
606 T3D in the presence DMSO or Z-VAD-FMK (25  $\mu$ M). Cell viability was assessed  
607 by Sytox green staining. \*,  $P < 0.05$  compared to DMSO treated cells of the same  
608 genotype. (D) BMDMs from wild-type, RIP3  $-/-$ , or Casp8  $-/-$  x RIP3  $-/-$  mice were  
609 infected with 50 PFU/cell of T3D. Cell death 48 h following infection was  
610 assessed by Cell Titer Glo. Luminescence measurement in mock-infected cells  
611 of the same genotype was considered to represent 100% viability. \*,  $P < 0.05$   
612 compared to wild-type cells. (E) BMDMs from wild-type or RIP3  $-/-$  mice were

613 infected with 50 PFU/cell of T3D in the presence or absence of Z-VAD-FMK (25  
614  $\mu$ M). Virus yield 24 h following infection was measured using plaque assay.

615

616 **Figure 3. Reovirus RNA is sufficient for the induction of necroptosis.** (A,B)

617 L929 cells were transfected with 100 ng of RNA extracted from mock-infected or  
618 reovirus-infected cells. (A) Cell death 24 h following transfection was assessed

619 by Cell Titer Glo. Luminescence measurement in untransfected cells was

620 considered to represent 100% viability. \*,  $P < 0.05$  compared to cells transfected

621 with RNA extracted from mock-infected cells. (B) Cell death 24 h following

622 transfection of RNA was assessed by AOEB staining. \*,  $P < 0.05$  compared to

623 cells transfected with RNA extracted from mock-infected cells (C) L929 cells

624 were transfected with 100 ng of RNA extracted from mock infected or reovirus-

625 infected cells in the presence of DMSO, Q-VD-OPh (25  $\mu$ M) or Nec1 (50  $\mu$ M).

626 Cell death 24 h following transfection was assessed by Cell Titer Glo.

627 Luminescence measurement in similarly treated cells transfected with RNA from

628 mock-infected cells was considered to represent 100% viability. \*,  $P < 0.05$

629 compared to cells transfected with DMSO treated cells transfected with the same

630 type of RNA (D) L929 cells were transfected with 100 ng of RNA extracted from

631 mock-infected or reovirus-infected cells. Levels of IFN $\beta$  mRNA were assessed by

632 RT-qPCR at 18 h following transfection. IFN $\beta$ :GAPDH ratio for cells transfected

633 with RNA from mock-infected cells was considered 1. \*,  $P < 0.05$  compared to

634 cells transfected with RNA from mock-infected cells. (E) L929 cells were

635 transfected with 100 ng of RNA extracted from mock-infected or reovirus-infected

636 cells in the presence and absence of 0.1  $\mu\text{g/ml}$  anti-IFNAR Ab. Cell death 24 h  
637 following transfection was assessed by Cell Titer Glo. Luminescence  
638 measurement in similarly treated cells transfected with RNA from mock-infected  
639 cells was considered to represent 100% viability. \*,  $P < 0.05$  compared to cells  
640 transfected with same type of RNA without anti-IFNAR Ab. (F) L929 cells were  
641 transfected 100 ng of untreated or CIP-treated RNA extracted from reovirus-  
642 infected cells. Levels of IFN $\beta$  mRNA were assessed by RT-qPCR at 18 h  
643 following transfection. IFN $\beta$ :GAPDH ratio for cells transfected with untreated  
644 RNA from reovirus-infected cells was considered 1. \*,  $P < 0.05$  compared to cells  
645 transfected with untreated RNA from reovirus-infected cells. (G) Cells treated  
646 with 0 or 100 units/ml IFN $\beta$  were transfected with 100 ng of untreated RNA from  
647 mock-infected cells or untreated or CIP-treated RNA from T3D-infected cells. Cell  
648 death 24 h following transfection was assessed by Cell Titer Glo. Luminescence  
649 measurement in similarly treated cells transfected with RNA from mock-infected  
650 cells was considered to represent 100% viability. \*,  $P < 0.05$  compared to  
651 similarly treated cells transfected with untreated RNA from T3D-infected cells. \*\*,  
652  $P < 0.05$  compared to cells transfected with similarly treated RNA in the presence  
653 of 0 units/ml of IFN $\beta$ . (H) Cells treated with 0 or 100 units/ml IFN $\beta$  were  
654 transfected with 100 ng of untreated or CIP-treated RNA from T3D-infected cells.  
655 Cell death 24 h following transfection of RNA was assessed by AOEB staining. \*,  
656  $P < 0.05$  compared to cells transfected with similarly treated RNA in the presence  
657 of 0 mU/ml of IFN $\beta$ . (I) Cells pretreated with 0 or 20 mM AC were transfected  
658 with RNA from T3D-infected cells. Levels of IFN $\beta$  mRNA were assessed by RT-

659 qPCR at 18 h following transfection. IFN $\beta$ :GAPDH ratio for cells 0 mM AC treated  
660 cells transfected with RNA from T3D-infected cells was considered 1. (J) Cells  
661 pretreated with 0 or 20 mM AC were transfected with 100 ng RNA from mock-  
662 infected or T3D-infected cells. Cell death 24 h following transfection was  
663 assessed by Cell Titer Glo. Luminescence measurement in similarly treated cells  
664 transfected with RNA from mock-infected cells was considered to represent  
665 100% viability. \*,  $P < 0.05$  compared to transfection of cells treated with 0 mM  
666 AC.

667

668 **Figure 4. Detection of viral RNA by cytoplasmic sensors is required for**  
669 **necroptosis.** (A) L929 cells were transfected with non-targeting siRNAs or  
670 siRNAs specific for RIG-I, MDA5, or MAVS. Efficiency of knockdown was  
671 assessed by immunoblotting for RIG-I, MDA5, MAVS and KDEL or PSTAIR  
672 loading controls. (B, C, D) L929 cells were transfected with non-targeting siRNAs  
673 or siRNAs specific for both RIG-I and MDA5, or MAVS. (B) Cell death 48 h  
674 following mock infection or infection with 10 PFU/cell of T3D was assessed by  
675 Cell Titer Glo. Luminescence measurement in uninfected cells transfected with  
676 the same siRNA was considered to represent 100% viability. \*,  $P < 0.05$   
677 compared to cells transfected with non-targeting siRNAs. (C) Cell death 48 h  
678 following infection with 10 PFU/cell of T3D was assessed by AOEB staining. \*,  $P$   
679  $< 0.05$  compared to cells transfected with non-targeting siRNAs. (D) Cell death 3  
680 h following treatment with TNF $\alpha$  and Z-VAD-FMK treatment was assessed by  
681 Cell Titer Glo. Luminescence measurement in similarly siRNA treated, DMSO

682 treated cells was considered to represent 100% viability. (E) Cell death in wild-  
683 type, RIG-I *-/-* x MDA5 *-/-* or MAVS *-/-* BMDMs treated with Z-VAD-FMK following  
684 mock infection or infection with 50 PFU/cell of T3D was assessed by Cell Titer  
685 Glo. Luminescence measurement in mock-infected cells of the same genotype  
686 was considered to represent 100% viability. \*,  $P < 0.05$  compared to wild-type  
687 cells. (F) Cell death in wild-type, RIG-I *-/-* x MDA5 *-/-* or MAVS *-/-* BMDMs treated  
688 with Z-VAD-FMK (25  $\mu$ M) following infection with 50 PFU/cell of T3D was  
689 assessed by Sytox green staining. \*,  $P < 0.05$  compared to wild-type cells.

690

691 **Figure 5. Signaling via IFNAR is required for necroptosis** (A,B,C,D) L929  
692 cells were infected with 10 PFU/cell of T3D in the presence of 0.1  $\mu$ g/ml of anti-  
693 IFNAR Ab. (A) Levels of ZBP1 mRNA were assessed using RT-qPCR at 24 h  
694 post infection. ZBP1:GAPDH ratio at 0 h post infection was set to 1. \*,  $P < 0.05$   
695 compared to cells infected without IFNAR antibody. (B) Cell death 48 h following  
696 mock infection or infection with 10 PFU/cell of T3D was assessed by Cell Titer  
697 Glo. Luminescence measurement in similarly treated, mock-infected cells was  
698 considered to represent 100% viability. \*,  $P < 0.05$  compared to cells infected  
699 without IFNAR antibody. (C) Cell death 48 h following infection with 10 PFU/cell  
700 of T3D was assessed by AOEB staining. \*,  $P < 0.05$  compared to cells infected  
701 without IFNAR antibody. (D) Viral infectivity 18 h following infection with 2  
702 PFU/cell T3D was assessed by indirect immunofluorescence. (E) Cell death 3 h  
703 following treatment with TNF $\alpha$  and Z-VAD-FMK treatment was assessed by Cell  
704 Titer Glo. Luminescence measurement cells treated without IFNAR antibody was

705 considered to represent 100% viability. (F) Cell death in wild-type and IFNAR-  
706 deficient BMDMs treated with Z-VAD-FMK following mock infection or infection  
707 with 50 PFU/cell of T3D. Cell viability was assessed by Cell titer Glo.  
708 Luminescence measurement in mock-infected cells of the same genotype was  
709 considered to represent 100% viability. \*,  $P < 0.05$  compared to wild-type cells.  
710 (G) Cell death in wild-type and IFNAR-deficient BMDMs treated with Z-VAD-FMK  
711 following infection with 50 PFU/cell of T3D was assessed by Sytox green  
712 staining. \*,  $P < 0.05$  compared to wild-type cells. (H) L929 cells were mock  
713 infected or infected with 100 PFU/cell of T3D ISVPs in the presence or absence  
714 of 20 mM AC. Cell death 48 h following infection was assessed by Cell Titer Glo.  
715 Luminescence measurement in similarly treated, mock-infected cells was  
716 considered to represent 100% viability. \*,  $P < 0.05$  compared to cells infected  
717 without AC. (H, I) L929 cells were transfected with non-targeting siRNAs or  
718 siRNAs specific for TRIF. (H) Efficiency of knockdown was assessed by  
719 immunoblotting for TRIF and PSTAIR loading control. (I) Cell death 48 h  
720 following mock infection or infection with 10 PFU/cell of T3D was assessed by  
721 Cell Titer Glo. Luminescence measurement in uninfected cells transfected with  
722 the same siRNA was considered to represent 100% viability.

723

724 **Figure 6. Synthesis for genomic dsRNA is required for necroptosis.** L929  
725 cells were infected with 10 PFU/cell of T3D in the presence of ribavirin (200  $\mu$ M)  
726 or GuHCl (15 mM). (A) Levels of reovirus + strand RNA corresponding to the viral  
727 S1 gene segment were measured by RT-qPCR 24 h post infection. Reovirus

728 T3D S1 +:GAPDH ratio in untreated cells infected for 0 h was considered 1. \*,  $P <$   
729 0.05 compared to cells infected with T3D in absence of inhibitor. (B) Levels of  
730 reovirus  $\mu$ 1C protein and PSTAIR loading control 24 h following infection with 10  
731 PFU/cell of T3D were assessed by immunoblotting. (C) Generation of reovirus  
732 genomic dsRNA at 24 h following infection was evaluated by electropherotyping.  
733 (D) Cell death 48 h following mock infection or infection with 10 PFU/cell of T3D  
734 was assessed by Cell Titer Glo. Luminescence measurement in similarly treated,  
735 uninfected cells was considered to represent 100% viability. \*,  $P <$  0.05  
736 compared to control treated cells. (E) Cell death 48 h following infection with 10  
737 PFU/cell of T3D was assessed by AOEB staining. \*,  $P <$  0.05 compared to  
738 control treated cells. (F) Cell death 4 h following treatment with  $\text{TNF}\alpha$  and Z-  
739 VAD-FMK treatment was assessed by Cell Titer Glo. Cell viability in similarly  
740 treated cells in absence of  $\text{TNF}\alpha$  and Z-VAD-FMK was considered 100%.

741

742 **Figure 7. De novo synthesis of viral RNA is not required for IFN expression.**

743 (A) L929 cells were infected with 10 PFU/cell of T3D. Levels of IFN $\beta$  mRNA were  
744 assessed at the indicated time intervals using RT-qPCR. IFN $\beta$ :GAPDH ratio at 0  
745 h post infection was set to 1. \*,  $P <$  0.05 compared to cells infected for 0 h. (B)  
746 L929 cells treated with AC (20 mM), ribavirin (200  $\mu$ M), or GuHCl (15 mM) were  
747 infected with 10 PFU/cell of T3D. Levels of IFN $\beta$  mRNA were assessed by RT-  
748 qPCR at 24 h post infection. IFN $\beta$ :GAPDH ratio for untreated, T3D-infected cells  
749 was set to 1. \*,  $P <$  0.05 compared to control treated, infected cells. (C,D) L929  
750 cells were infected with 10 PFU/cell of T3D and equivalent particles of UV-

751 treated T3D. (C) Levels of reovirus + strand RNA corresponding to the viral S1  
752 gene segment were measured by RT-qPCR 24 h post infection. Reovirus T3D  
753 S1 +:GAPDH ratio in cells infected for 0 h was considered 1. UD, undetectable,  
754 value below that detected at 0 h (D) Levels of reovirus IFN $\beta$  RNA corresponding  
755 were measured by RT-qPCR 24 h post infection. IFN $\beta$ :GAPDH ratio in cells  
756 infected with infectious T3D was considered 1. (E) L929 cells were transfected  
757 with non-targeting siRNAs or siRNAs specific for MAVS. Levels of IFN $\beta$  mRNA in  
758 cells infected with 10 PFU/cell of T3D in the presence of absence of ribavirin  
759 (200  $\mu$ M) were assessed by RT-qPCR. IFN $\beta$ :GAPDH ratio for untreated, T3D  
760 infected non-targeting siRNA treated was set to 1. \*,  $P < 0.05$  compared to  
761 untreated, T3D infected non-targeting siRNA treated cells.

762

763 **Figure 8. Model for reovirus-induced necroptosis.** Genomic RNA from  
764 incoming viral particles is sensed by RLRs to produce type I IFN in a MAVS-  
765 dependent manner. De novo synthesized viral genomic dsRNA or viral  
766 secondary transcripts produced from newly synthesized genomic dsRNA (GuHCl  
767 sensitive replication events) are detected by an as yet unidentified ISG to elicit  
768 RIP3-dependent necrotic cell death.



## 769 REFERENCES

770

771

772

773

774

775

776

777

778

779

780

781

782

783

784

785

786

787

788

789

790

791

792

793

794

795

796

797

798

799

800

801

802

803

804

805

806

807

1. **Danthi P.** 2016. Viruses and the Diversity of Cell Death. *Annu Rev Virol* **3**:533-553.
2. **Wang X, Li Y, Liu S, Yu X, Li L, Shi C, He W, Li J, Xu L, Hu Z, Yu L, Yang Z, Chen Q, Ge L, Zhang Z, Zhou B, Jiang X, Chen S, He S.** 2014. Direct activation of RIP3/MLKL-dependent necrosis by herpes simplex virus 1 (HSV-1) protein ICP6 triggers host antiviral defense. *Proc Natl Acad Sci U S A* **111**:15438-15443.
3. **Huang Z, Wu SQ, Liang Y, Zhou X, Chen W, Li L, Wu J, Zhuang Q, Chen C, Li J, Zhong CQ, Xia W, Zhou R, Zheng C, Han J.** 2015. RIP1/RIP3 binding to HSV-1 ICP6 initiates necroptosis to restrict virus propagation in mice. *Cell Host Microbe* **17**:229-242.
4. **Upton JW, Kaiser WJ, Mocarski ES.** 2010. Virus inhibition of RIP3-dependent necrosis. *Cell host & microbe* **7**:302-313.
5. **Upton JW, Kaiser WJ, Mocarski ES.** 2012. DAI/ZBP1/DLM-1 complexes with RIP3 to mediate virus-induced programmed necrosis that is targeted by murine cytomegalovirus vIRA. *Cell Host Microbe* **11**:290-297.
6. **Cho YS, Challa S, Moquin D, Genga R, Ray TD, Guildford M, Chan FK.** 2009. Phosphorylation-driven assembly of the RIP1-RIP3 complex regulates programmed necrosis and virus-induced inflammation. *Cell* **137**:1112-1123.
7. **Nogusa S, Thapa RJ, Dillon CP, Liedmann S, Oguin TH, 3rd, Ingram JP, Rodriguez DA, Kosoff R, Sharma S, Sturm O, Verbist K, Gough PJ, Bertin J, Hartmann BM, Sealfon SC, Kaiser WJ, Mocarski ES, Lopez CB, Thomas PG, Oberst A, Green DR, Balachandran S.** 2016. RIPK3 Activates Parallel Pathways of MLKL-Driven Necroptosis and FADD-Mediated Apoptosis to Protect against Influenza A Virus. *Cell Host Microbe* **20**:13-24.
8. **Rodrigue-Gervais IG, Labbe K, Dagenais M, Dupaul-Chicoine J, Champagne C, Morizot A, Skeldon A, Brincks EL, Vidal SM, Griffith TS, Saleh M.** 2014. Cellular inhibitor of apoptosis protein cIAP2 protects against pulmonary tissue necrosis during influenza virus infection to promote host survival. *Cell Host Microbe* **15**:23-35.
9. **Chan FK.** 2012. Fueling the flames: Mammalian programmed necrosis in inflammatory diseases. *Cold Spring Harb Perspect Biol* **4**.
10. **Mocarski ES, Kaiser WJ, Livingston-Rosanoff D, Upton JW, Daley-Bauer LP.** 2014. True grit: programmed necrosis in antiviral host defense, inflammation, and immunogenicity. *J Immunol* **192**:2019-2026.

- 808 11. **Zhang DW, Shao J, Lin J, Zhang N, Lu BJ, Lin SC, Dong MQ, Han J.**  
809 2009. RIP3, an energy metabolism regulator that switches TNF-induced  
810 cell death from apoptosis to necrosis. *Science* **325**:332-336.
- 811 12. **He S, Wang L, Miao L, Wang T, Du F, Zhao L, Wang X.** 2009. Receptor  
812 interacting protein kinase-3 determines cellular necrotic response to TNF-  
813 alpha. *Cell* **137**:1100-1111.
- 814 13. **Wang H, Sun L, Su L, Rizo J, Liu L, Wang LF, Wang FS, Wang X.**  
815 2014. Mixed lineage kinase domain-like protein MLKL causes necrotic  
816 membrane disruption upon phosphorylation by RIP3. *Mol Cell* **54**:133-146.
- 817 14. **Zhao J, Jitkaew S, Cai Z, Choksi S, Li Q, Luo J, Liu ZG.** 2012. Mixed  
818 lineage kinase domain-like is a key receptor interacting protein 3  
819 downstream component of TNF-induced necrosis. *Proceedings of the*  
820 *National Academy of Sciences of the United States of America* **109**:5322-  
821 5327.
- 822 15. **Galluzzi L, Vitale I, Abrams JM, Alnemri ES, Baehrecke EH,**  
823 **Blagosklonny MV, Dawson TM, Dawson VL, El-Deiry WS, Fulda S,**  
824 **Gottlieb E, Green DR, Hengartner MO, Kepp O, Knight RA, Kumar S,**  
825 **Lipton SA, Lu X, Madeo F, Malorni W, Mehlen P, Nunez G, Peter ME,**  
826 **Piacentini M, Rubinsztein DC, Shi Y, Simon HU, Vandenabeele P,**  
827 **White E, Yuan J, Zhivotovsky B, Melino G, Kroemer G.** 2012.  
828 Molecular definitions of cell death subroutines: recommendations of the  
829 Nomenclature Committee on Cell Death 2012. *Cell Death Differ* **19**:107-  
830 120.
- 831 16. **Sun L, Wang H, Wang Z, He S, Chen S, Liao D, Wang L, Yan J, Liu W,**  
832 **Lei X, Wang X.** 2012. Mixed lineage kinase domain-like protein mediates  
833 necrosis signaling downstream of RIP3 kinase. *Cell* **148**:213-227.
- 834 17. **Quarato G, Guy CS, Grace CR, Llambi F, Nourse A, Rodriguez DA,**  
835 **Wakefield R, Frase S, Moldoveanu T, Green DR.** 2016. Sequential  
836 Engagement of Distinct MLKL Phosphatidylinositol-Binding Sites Executes  
837 Necroptosis. *Mol Cell* **61**:589-601.
- 838 18. **Murphy JM, Czabotar PE, Hildebrand JM, Lucet IS, Zhang JG,**  
839 **Alvarez-Diaz S, Lewis R, Lalaoui N, Metcalf D, Webb AI, Young SN,**  
840 **Varghese LN, Tannahill GM, Hatchell EC, Majewski IJ, Okamoto T,**  
841 **Dobson RC, Hilton DJ, Babon JJ, Nicola NA, Strasser A, Silke J,**  
842 **Alexander WS.** 2013. The Pseudokinase MLKL Mediates Necroptosis via  
843 a Molecular Switch Mechanism. *Immunity* **39**:443-453.
- 844 19. **Moujalled DM, Cook WD, Murphy JM, Vaux DL.** 2014. Necroptosis  
845 induced by RIPK3 requires MLKL but not Drp1. *Cell Death Dis* **5**:e1086.

- 846 20. **Hildebrand JM, Tanzer MC, Lucet IS, Young SN, Spall SK, Sharma P,**  
847 **Pierotti C, Garnier JM, Dobson RC, Webb AI, Tripaydonis A, Babon**  
848 **JJ, Mulcair MD, Scanlon MJ, Alexander WS, Wilks AF, Czabotar PE,**  
849 **Lessene G, Murphy JM, Silke J.** 2014. Activation of the pseudokinase  
850 MLKL unleashes the four-helix bundle domain to induce membrane  
851 localization and necroptotic cell death. *Proc Natl Acad Sci U S A*  
852 **111:15072-15077.**
- 853 21. **Galluzzi L, Kepp O, Kroemer G.** 2014. MLKL regulates necrotic plasma  
854 membrane permeabilization. *Cell Res* **24:139-140.**
- 855 22. **Dondelinger Y, Declercq W, Montessuit S, Roelandt R, Goncalves A,**  
856 **Bruggeman I, Hulpiau P, Weber K, Sehon CA, Marquis RW, Bertin J,**  
857 **Gough PJ, Savvides S, Martinou JC, Bertrand MJ, Vandenabeele P.**  
858 2014. MLKL compromises plasma membrane integrity by binding to  
859 phosphatidylinositol phosphates. *Cell Rep* **7:971-981.**
- 860 23. **Cai Z, Jitkaew S, Zhao J, Chiang HC, Choksi S, Liu J, Ward Y, Wu LG,**  
861 **Liu ZG.** 2014. Plasma membrane translocation of trimerized MLKL protein  
862 is required for TNF-induced necroptosis. *Nat Cell Biol* **16:55-65.**
- 863 24. **Newton K.** 2015. RIPK1 and RIPK3: critical regulators of inflammation  
864 and cell death. *Trends Cell Biol* **25:347-353.**
- 865 25. **Kaiser WJ, Sridharan H, Huang C, Mandal P, Upton JW, Gough PJ,**  
866 **Sehon CA, Marquis RW, Bertin J, Mocarski ES.** 2013. Toll-like receptor  
867 3-mediated necrosis via TRIF, RIP3, and MLKL. *J Biol Chem* **288:31268-**  
868 **31279.**
- 869 26. **He S, Liang Y, Shao F, Wang X.** 2011. Toll-like receptors activate  
870 programmed necrosis in macrophages through a receptor-interacting  
871 kinase-3-mediated pathway. *Proc Natl Acad Sci U S A* **108:20054-20059.**
- 872 27. **Kuriakose T, Man, S.M., Malireddi, R.S., Karki, R., Kesavardhana, S.,**  
873 **Place, D.E., Neale, G., Vogel, P. and Kanneganti, T.D.** 2016. ZBP1/DAI  
874 is an innate sensor of influenza virus triggering the NLRP3 inflammasome  
875 and programmed cell death pathways. *Science Immunology* **1:aag2045.**
- 876 28. **Thapa RJ, Ingram JP, Ragan KB, Nogusa S, Boyd DF, Benitez AA,**  
877 **Sridharan H, Kosoff R, Shubina M, Landsteiner VJ, Andrade M, Vogel**  
878 **P, Sigal LJ, tenOever BR, Thomas PG, Upton JW, Balachandran S.**  
879 2016. DAI Senses Influenza A Virus Genomic RNA and Activates RIPK3-  
880 Dependent Cell Death. *Cell Host Microbe*  
881 doi:10.1016/j.chom.2016.09.014.
- 882 29. **Bozym RA, Patel K, White C, Cheung KH, Bergelson JM, Morosky SA,**  
883 **Coyne CB.** 2011. Calcium signals and calpain-dependent necrosis are

- 884 essential for release of coxsackievirus B from polarized intestinal epithelial  
885 cells. *Mol Biol Cell* **22**:3010-3021.
- 886 30. **Berger AK, Danthi P.** 2013. Reovirus activates a caspase-independent  
887 cell death pathway. *mBio* **4**.
- 888 31. **Chu JJ, Ng ML.** 2003. The mechanism of cell death during West Nile  
889 virus infection is dependent on initial infectious dose. *J Gen Virol* **84**:3305-  
890 3314.
- 891 32. **Meessen-Pinard M, Le Coupanec A, Desforges M, Talbot PJ.** 2016.  
892 Pivotal role of RIP1 and MLKL in neuronal cell death induced by the  
893 human neuroinvasive coronavirus OC43. *J Virol* doi:10.1128/JVI.01513-  
894 16.
- 895 33. **Kobayashi T, Antar AAR, Boehme KW, Danthi P, Eby EA, Guglielmi  
896 KM, Holm GH, Johnson EM, Maginnis MS, Naik S, Skelton WB,  
897 Wetzel JD, Wilson GJ, Chappell JD, Dermody TS.** 2007. A plasmid-  
898 based reverse genetics system for animal double-stranded RNA viruses.  
899 *Cell Host Microbe* **1**:147-157.
- 900 34. **Danthi P, Kobayashi T, Holm GH, Hansberger MW, Abel TW,  
901 Dermody TS.** 2008. Reovirus apoptosis and virulence are regulated by  
902 host cell membrane penetration efficiency. *J Virol* **82**:161-172.
- 903 35. **Berard A, Coombs KM.** 2009. Mammalian reoviruses: propagation,  
904 quantification, and storage. *Curr Protoc Microbiol* **Chapter 15**:Unit15C 11.
- 905 36. **Virgin HW, IV, Bassel-Duby R, Fields BN, Tyler KL.** 1988. Antibody  
906 protects against lethal infection with the neurally spreading reovirus type 3  
907 (Dearing). *Journal of Virology* **62**:4594-4604.
- 908 37. **Wu YT, Tan HL, Huang Q, Sun XJ, Zhu X, Shen HM.** 2011. zVAD-  
909 induced necroptosis in L929 cells depends on autocrine production of  
910 TNFalpha mediated by the PKC-MAPKs-AP-1 pathway. *Cell death and  
911 differentiation* **18**:26-37.
- 912 38. **Holler N, Zaru R, Micheau O, Thome M, Attinger A, Valitutti S,  
913 Bodmer JL, Schneider P, Seed B, Tschopp J.** 2000. Fas triggers an  
914 alternative, caspase-8-independent cell death pathway using the kinase  
915 RIP as effector molecule. *Nat Immunol* **1**:489-495.
- 916 39. **Becker MM, Peters TR, Dermody TS.** 2003. Reovirus sigma NS and mu  
917 NS proteins form cytoplasmic inclusion structures in the absence of viral  
918 infection. *J Virol* **77**:5948-5963.
- 919 40. **Reynolds ES.** 1963. The use of lead citrate at high pH as an electron-  
920 opaque stain in electron microscopy. *J Cell Biol* **17**:208-212.

- 921 41. **Tyler KL, Squier MK, Rodgers SE, Schneider BE, Oberhaus SM,**  
922 **Grdina TA, Cohen JJ, Dermody TS.** 1995. Differences in the capacity of  
923 reovirus strains to induce apoptosis are determined by the viral  
924 attachment protein sigma 1. *J Virol* **69**:6972-6979.
- 925 42. **Schmittgen TD, Livak KJ.** 2008. Analyzing real-time PCR data by the  
926 comparative C(T) method. *Nat Protoc* **3**:1101-1108.
- 927 43. **Vanden Berghe T, Grootjans S, Goossens V, Dondelinger Y, Krysko**  
928 **DV, Takahashi N, Vandenabeele P.** 2013. Determination of apoptotic  
929 and necrotic cell death in vitro and in vivo. *Methods* **61**:117-129.
- 930 44. **Newton K, Dugger DL, Wickliffe KE, Kapoor N, de Almagro MC, Vucic**  
931 **D, Komuves L, Ferrando RE, French DM, Webster J, Roose-Girma M,**  
932 **Warming S, Dixit VM.** 2014. Activity of protein kinase RIPK3 determines  
933 whether cells die by necroptosis or apoptosis. *Science* **343**:1357-1360.
- 934 45. **Mandal P, Berger SB, Pillay S, Moriwaki K, Huang C, Guo H, Lich JD,**  
935 **Finger J, Kasparcova V, Votta B, Ouellette M, King BW, Wisnoski D,**  
936 **Lakdawala AS, DeMartino MP, Casillas LN, Haile PA, Sehon CA,**  
937 **Marquis RW, Upton J, Daley-Bauer LP, Roback L, Ramia N, Dovey**  
938 **CM, Carette JE, Chan FK, Bertin J, Gough PJ, Mocarski ES, Kaiser**  
939 **WJ.** 2014. RIP3 induces apoptosis independent of pronecrotic kinase  
940 activity. *Mol Cell* **56**:481-495.
- 941 46. **Rodriguez DA, Weinlich R, Brown S, Guy C, Fitzgerald P, Dillon CP,**  
942 **Oberst A, Quarato G, Low J, Cripps JG, Chen T, Green DR.** 2016.  
943 Characterization of RIPK3-mediated phosphorylation of the activation loop  
944 of MLKL during necroptosis. *Cell Death Differ* **23**:76-88.
- 945 47. **Connolly JL, Rodgers SE, Clarke P, Ballard DW, Kerr LD, Tyler KL,**  
946 **Dermody TS.** 2000. Reovirus-induced apoptosis requires activation of  
947 transcription factor NF-kappaB. *J Virol* **74**:2981-2989.
- 948 48. **Danthi P, Pruijssers AJ, Berger AK, Holm GH, Zinkel SS, Dermody**  
949 **TS.** 2010. Bid regulates the pathogenesis of neurotropic reovirus. *PLoS*  
950 *Pathog* **6**:e1000980.
- 951 49. **Holm GH, Zurney J, Tumilasci V, Leveille S, Danthi P, Hiscott J,**  
952 **Sherry B, Dermody TS.** 2007. Retinoic acid-inducible gene-I and  
953 interferon-beta promoter stimulator-1 augment proapoptotic responses  
954 following mammalian reovirus infection via interferon regulatory factor-3. *J*  
955 *Biol Chem* **282**:21953-21961.
- 956 50. **Prujssers AJ, Hengel H, Abel TW, Dermody TS.** 2013. Apoptosis  
957 induction influences reovirus replication and virulence in newborn mice. *J*  
958 *Virol* **87**:12980-12989.

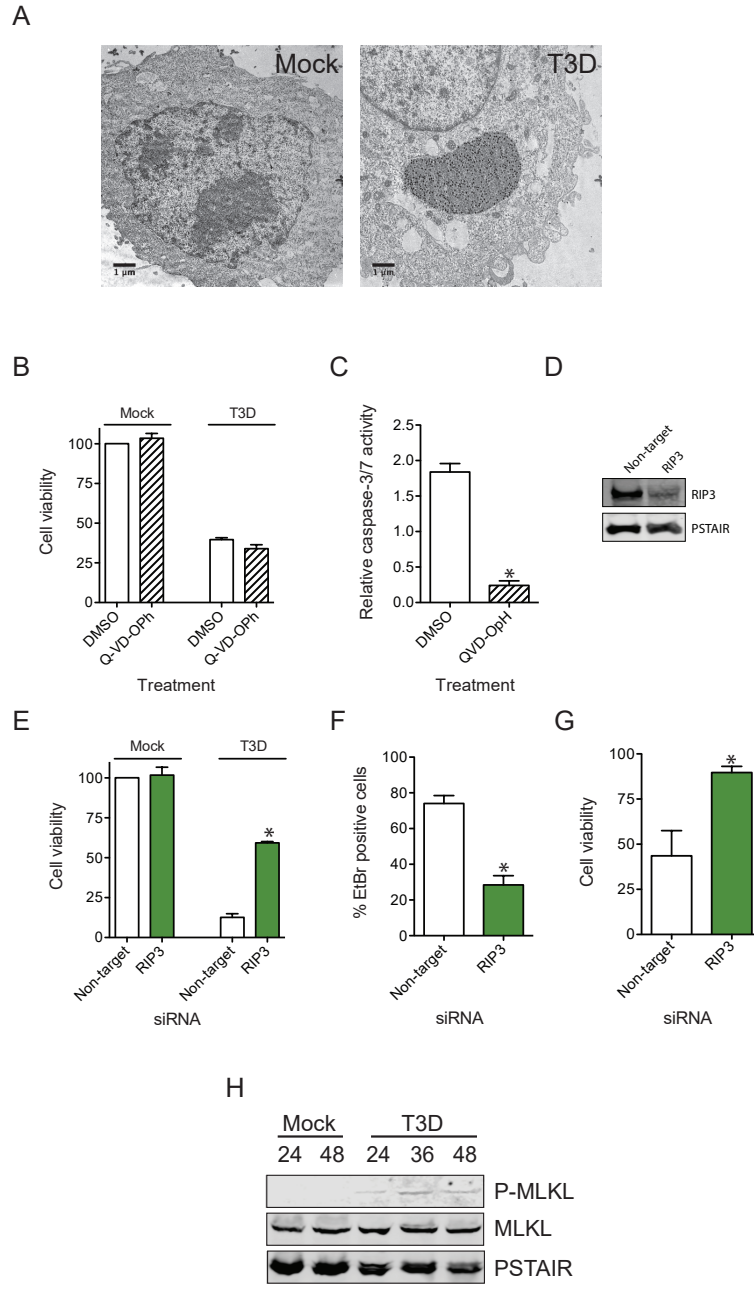
- 959 51. **Clarke P, Beckham JD, Leser JS, Hoyt CC, Tyler KL.** 2009. Fas-  
960 mediated apoptotic signaling in the mouse brain following reovirus  
961 infection. *J Virol* **83**:6161-6170.
- 962 52. **Berens HM, Tyler KL.** 2011. The proapoptotic Bcl-2 protein Bax plays an  
963 important role in the pathogenesis of reovirus encephalitis. *Journal of*  
964 *virology* **85**:3858-3871.
- 965 53. **Dionne KR, Zhuang Y, Leser JS, Tyler KL, Clarke P.** 2013. Daxx  
966 upregulation within the cytoplasm of reovirus-infected cells is mediated by  
967 interferon and contributes to apoptosis. *J Virol* **87**:3447-3460.
- 968 54. **Zhuang Y, Berens-Norman HM, Leser JS, Clarke P, Tyler KL.** 2016.  
969 Mitochondrial p53 Contributes to Reovirus-Induced Neuronal Apoptosis  
970 and Central Nervous System Injury in a Mouse Model of Viral  
971 Encephalitis. *J Virol* **90**:7684-7691.
- 972 55. **Gunther C, Martini E, Wittkopf N, Amann K, Weigmann B, Neumann**  
973 **H, Waldner MJ, Hedrick SM, Tenzer S, Neurath MF, Becker C.** 2011.  
974 Caspase-8 regulates TNF-alpha-induced epithelial necroptosis and  
975 terminal ileitis. *Nature* **477**:335-339.
- 976 56. **Kaiser WJ, Upton JW, Long AB, Livingston-Rosanoff D, Daley-Bauer**  
977 **LP, Hakem R, Caspary T, Mocarski ES.** 2011. RIP3 mediates the  
978 embryonic lethality of caspase-8-deficient mice. *Nature* **471**:368-372.
- 979 57. **Oberst A, Dillon CP, Weinlich R, McCormick LL, Fitzgerald P, Pop C,**  
980 **Hakem R, Salvesen GS, Green DR.** 2011. Catalytic activity of the  
981 caspase-8-FLIP(L) complex inhibits RIPK3-dependent necrosis. *Nature*  
982 **471**:363-367.
- 983 58. **Hiller BE, Berger AK, Danthi P.** 2015. Viral gene expression potentiates  
984 reovirus-induced necrosis. *Virology* doi:10.1016/j.virol.2015.06.018.
- 985 59. **Kalai M, Van Loo G, Vanden Berghe T, Meeus A, Burm W, Saelens X,**  
986 **Vandenabeele P.** 2002. Tipping the balance between necrosis and  
987 apoptosis in human and murine cells treated with interferon and dsRNA.  
988 *Cell Death Differ* **9**:981-994.
- 989 60. **Goubau D, Schlee M, Deddouch S, Pruijssers AJ, Zillinger T,**  
990 **Goldeck M, Schuberth C, Van der Veen AG, Fujimura T, Rehwinkel J,**  
991 **Iskarpotyoti JA, Barchet W, Ludwig J, Dermody TS, Hartmann G, Reis**  
992 **ESC.** 2014. Antiviral immunity via RIG-I-mediated recognition of RNA  
993 bearing 5'-diphosphates. *Nature* doi:10.1038/nature13590.
- 994 61. **McAllister CS, Taghavi N, Samuel CE.** 2012. Protein kinase PKR  
995 amplification of interferon beta induction occurs through initiation factor  
996 eIF-2alpha-mediated translational control. *J Biol Chem* **287**:36384-36392.

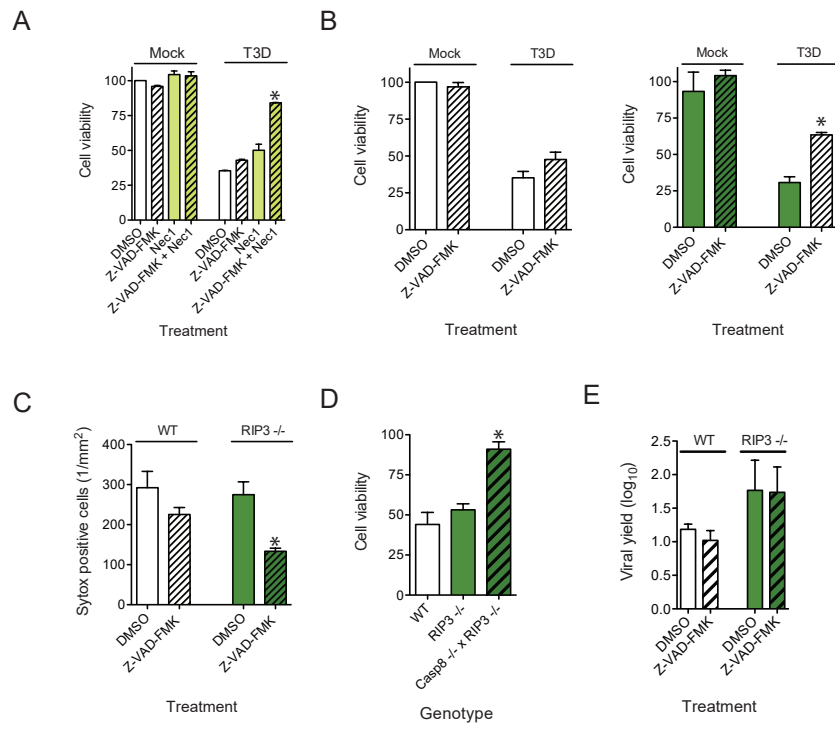
- 997 62. **Kato H, Takeuchi O, Mikamo-Satoh E, Hirai R, Kawai T, Matsushita K,**  
998 **Hiiragi A, Dermody TS, Fujita T, Akira S.** 2008. Length-dependent  
999 recognition of double-stranded ribonucleic acids by retinoic acid-inducible  
1000 gene-I and melanoma differentiation-associated gene 5. *J Exp Med*  
1001 **205**:1601-1610.
- 1002 63. **Sheehan KC, Lai KS, Dunn GP, Bruce AT, Diamond MS, Heutel JD,**  
1003 **Dungo-Arthur C, Carrero JA, White JM, Hertzog PJ, Schreiber RD.**  
1004 2006. Blocking monoclonal antibodies specific for mouse IFN-alpha/beta  
1005 receptor subunit 1 (IFNAR-1) from mice immunized by in vivo  
1006 hydrodynamic transfection. *J Interferon Cytokine Res* **26**:804-819.
- 1007 64. **de Bouteiller O, Merck E, Hasan UA, Hubac S, Benguigui B, Trinchieri**  
1008 **G, Bates EE, Caux C.** 2005. Recognition of double-stranded RNA by  
1009 human toll-like receptor 3 and downstream receptor signaling requires  
1010 multimerization and an acidic pH. *J Biol Chem* **280**:38133-38145.
- 1011 65. **Loo YM, Fornek J, Crochet N, Bajwa G, Perwitasari O, Martinez-**  
1012 **Sobrido L, Akira S, Gill MA, Garcia-Sastre A, Katze MG, Gale M, Jr.**  
1013 2008. Distinct RIG-I and MDA5 signaling by RNA viruses in innate  
1014 immunity. *J Virol* **82**:335-345.
- 1015 66. **Clarke P, Leser JS, Bowen RA, Tyler KL.** 2014. Virus-induced  
1016 transcriptional changes in the brain include the differential expression of  
1017 genes associated with interferon, apoptosis, interleukin 17 receptor A, and  
1018 glutamate signaling as well as flavivirus-specific upregulation of tRNA  
1019 synthetases. *MBio* **5**:e00902-00914.
- 1020 67. **Sturzenbecker LJ, Nibert ML, Furlong DB, Fields BN.** 1987.  
1021 Intracellular digestion of reovirus particles requires a low pH and is an  
1022 essential step in the viral infectious cycle. *Journal of Virology* **61**:2351-  
1023 2361.
- 1024 68. **Dermody TS, Parker JC, Sherry B.** 2013. Orthoreoviruses. *In* Knipe DM,  
1025 Howley PM (ed), *Fields Virology*, Sixth ed, vol 2. Lippincott Williams &  
1026 Wilkins, Philadelphia.
- 1027 69. **Murray KE, Nibert ML.** 2007. Guanidine hydrochloride inhibits  
1028 mammalian orthoreovirus growth by reversibly blocking the synthesis of  
1029 double-stranded RNA. *J Virol* **81**:4572-4584.
- 1030 70. **Henderson DR, Joklik WK.** 1978. The mechanism of interferon induction  
1031 by UV-irradiated reovirus. *Virology* **91**:389-406.
- 1032 71. **Lostale-Seijo I, Martinez-Costas J, Benavente J.** 2016. Interferon  
1033 induction by avian reovirus. *Virology* **487**:104-111.

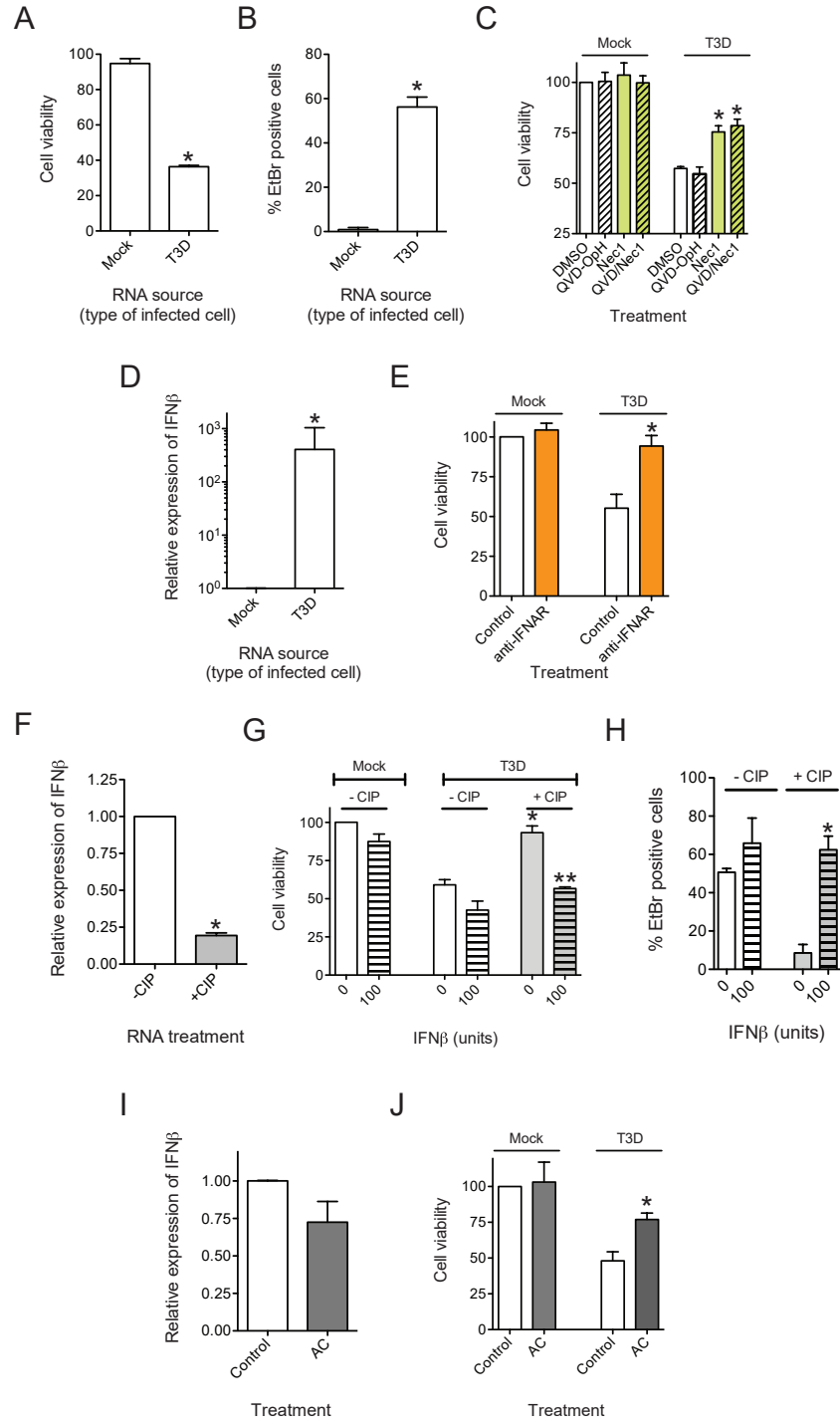
- 1034 72. **Robinson N, McComb S, Mulligan R, Dudani R, Krishnan L, Sad S.** 2012. Type I interferon induces necroptosis in macrophages during infection with *Salmonella enterica* serovar Typhimurium. *Nat Immunol* **13**:954-962.
- 1035  
1036  
1037
- 1038 73. **McComb S, Cessford E, Alturki NA, Joseph J, Shutinoski B, Startek JB, Gamero AM, Mossman KL, Sad S.** 2014. Type-I interferon signaling through ISGF3 complex is required for sustained Rip3 activation and necroptosis in macrophages. *Proc Natl Acad Sci U S A* doi:10.1073/pnas.1407068111.
- 1039  
1040  
1041  
1042
- 1043 74. **Thapa RJ, Nogusa S, Chen P, Maki JL, Lerro A, Andrade M, Rall GF, Degterev A, Balachandran S.** 2013. Interferon-induced RIP1/RIP3-mediated necrosis requires PKR and is licensed by FADD and caspases. *Proc Natl Acad Sci U S A* **110**:E3109-3118.
- 1044  
1045  
1046
- 1047 75. **Imani F, Jacobs BL.** 1988. Inhibitory activity for the interferon-induced protein kinase is associated with the reovirus serotype 1 sigma 3 protein. *Proceedings of the National Academy of Sciences of the United States of America* **85**:7887-7891.
- 1048  
1049  
1050
- 1051 76. **Connolly JL, Dermody TS.** 2002. Virion disassembly is required for apoptosis induced by reovirus. *J Virol* **76**:1632-1641.
- 1052
- 1053 77. **Danthi P, Coffey CM, Parker JS, Abel TW, Dermody TS.** 2008. Independent regulation of reovirus membrane penetration and apoptosis by the mu1 phi domain. *PLoS Pathog* **4**:e1000248.
- 1054  
1055
- 1056 78. **Knowlton JJ, Dermody TS, Holm GH.** 2012. Apoptosis induced by mammalian reovirus is beta interferon (IFN) independent and enhanced by IFN regulatory factor 3- and NF-kappaB-dependent expression of Noxa. *J Virol* **86**:1650-1660.
- 1057  
1058  
1059
- 1060 79. **Fensterl V, Chattopadhyay S, Sen GC.** 2015. No Love Lost Between Viruses and Interferons. *Annu Rev Virol* **2**:549-572.
- 1061
- 1062 80. **Zarbl H, Skup S, Millward S.** 1980. Reovirus progeny subviral particles synthesize uncapped mRNA. *Journal of Virology* **34**:497-505.
- 1063
- 1064 81. **Clarke P, Tyler KL.** 2009. Apoptosis in animal models of virus-induced disease. *Nat Rev Microbiol* **7**:144-155.
- 1065
- 1066 82. **O'Donnell SM, Hansberger MW, Connolly JL, Chappell JD, Watson MJ, Pierce JM, Wetzel JD, Han W, Barton ES, Forrest JC, Valyi-Nagy T, Yull FE, Blackwell TS, Rottman JN, Sherry B, Dermody TS.** 2005. Organ-specific roles for transcription factor NF-kappaB in reovirus-induced apoptosis and disease. *J Clin Invest* **115**:2341-2350.
- 1067  
1068  
1069  
1070

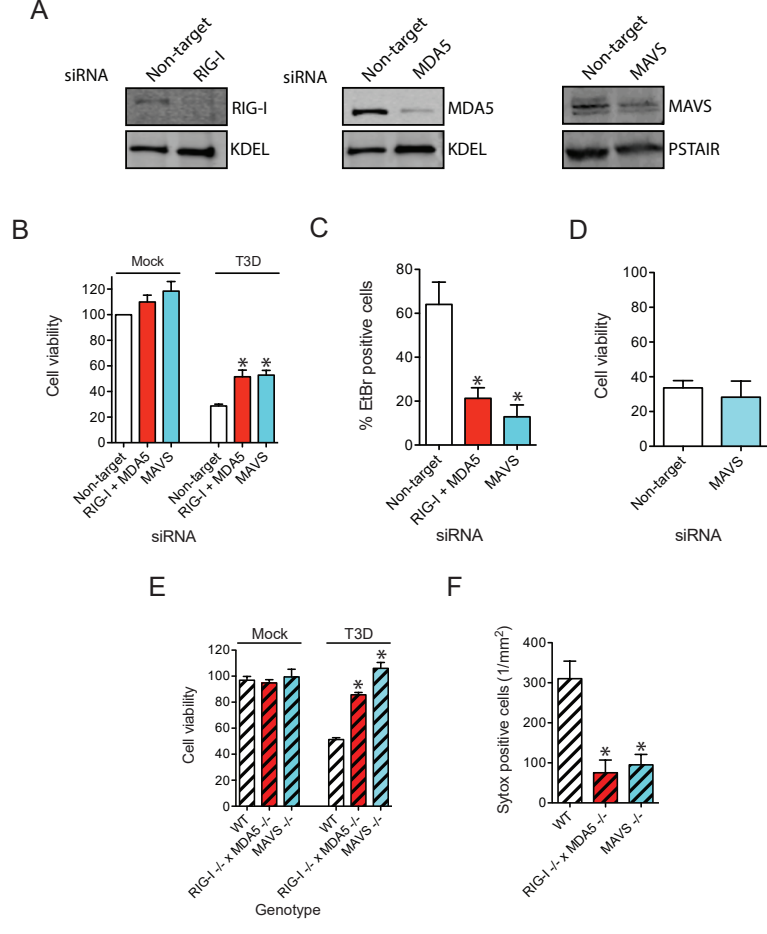


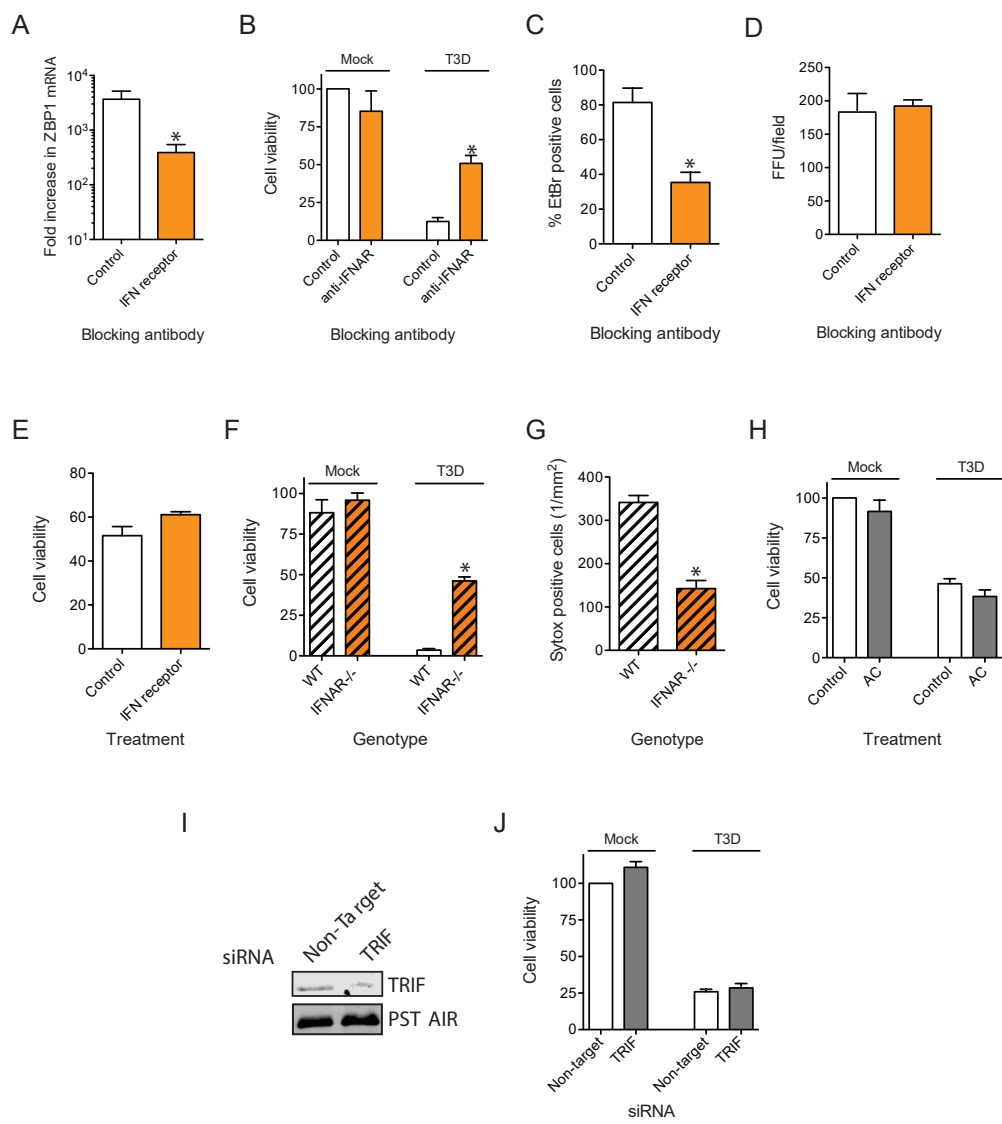
- 1071 83. **Holm GH, Pruijssers AJ, Li L, Danthi P, Sherry B, Dermody TS.** 2010.  
1072 Interferon regulatory factor 3 attenuates reovirus myocarditis and  
1073 contributes to viral clearance. *J Virol* **84**:6900-6908.
- 1074 84. **Maitra R, Ghalib MH, Goel S.** 2012. Reovirus: A Targeted Therapeutic -  
1075 Progress and Potential. *Mol Cancer Res* doi:10.1158/1541-7786.MCR-12-  
1076 0157.  
1077



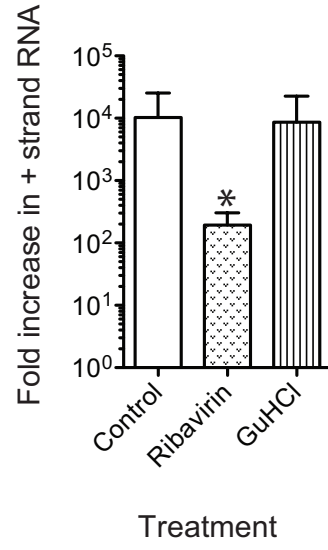




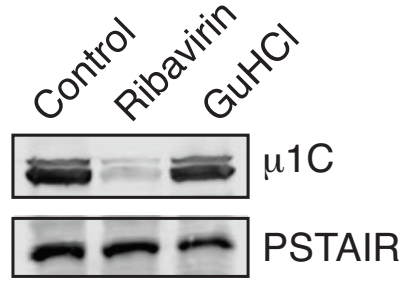




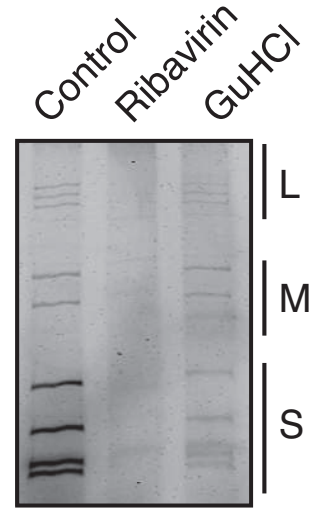
A



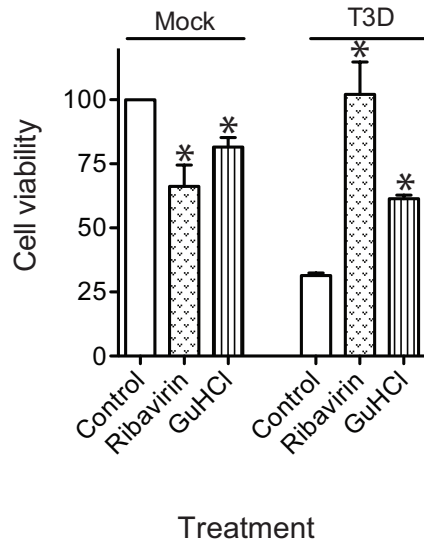
B



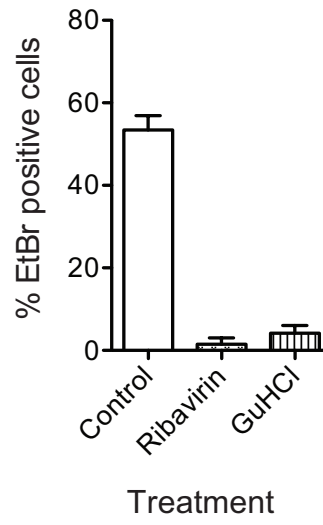
C



D



E



F

